Ann. Phys. (Leipzig) **8** (1999) 1, 83 – 110

Atomic interferometry as two-level particle scattering by a periodic potential

Christian J. Bordé[1,2 1] **and Claus Lämmerzahl**[1,3 2]

[1] Laboratoire de Physique des Lasers, Institut Galilée,
Université Paris 13, F-93430 Villetaneuse, France
[2] Laboratoire de Gravitation et Cosmologie Relativiste, Université Pierre et Marie Curie,
Tour 22, Boîte Courier 142, 4 Place Jussieu, F-75252 Cedex 05 Paris, France
[3] Fakultät für Physik, Universität Konstanz, Postfach 5560 M674, D-78457 Konstanz, Germany

Received 15 July 1998, accepted 9 October 1998 by F. W. Hehl

Abstract. The beam splitting process of an atomic beam is described by an exactly solvable theory. We use exact plane wave solutions of an atomic two-level system interacting with laser beams and employ appropriate jump conditions between regions with and without laser beam. The transmission matrix as well as the reflection matrix are given explicitely. Also, the conditions for atom optical analogues of the Borrmann effect and of the *pendellösung* effect are treated exactly. The high-energy limit of these phenomena is discussed which is sufficient for many practical purposes.

Keywords: Atomic interferometry; Atom-laser interaction; Beam splitter; Atom optics

1 Introduction

Atomic and molecular interferometry [1, 2, 3, 4, 5] proved to be very successful tools in probing the interaction of quantum objects with externals fields, e.g. with gravitational acceleration or rotation. These experiments are based on the theoretical framework developed in [6], for a review see [7]. The main part of such a device is the beam splitter. In order to give a correct interpretation of the experimental results it is necessary to give an appropriate description of the beam splitting process.

There are two versions of atomic beam splitters and correspondingly two versions of atom interferometers: the first uses a *stationary* interaction geometry with time-independent laser beams while the second uses laser *pulses*. The first case corresponds to a stationary, the second case to a time-dependent quantum mechanical problem. The latter problem has an exact solution, even in the case of an additional gravitational field [8, 9]. The purpose of this paper is to give an exact quantum mechanical description of the beam splitting process in the stationary case.

In doing so, we treat this problem as the scattering of an atomic beam by a periodic potential which is given by the laser beam. We proceed in the same gen-

---

[1] E-mail: chbo@ccr.jussieu.fr
[2] E-mail: claus.laemmerzahl@uni-konstanz.de

eral manner as in usual calculations of the transmission and reflection of a plane wave by a potential barrier. However, in our case the problem is more complicated due to the two-level structure of the quantum state and the periodic structure of the scattering potential. The transmitted as well as the reflected atoms are, in general, found to be in a superposition of the excited and ground state even if they are, for example, only in the ground state in front of the laser beam. Since the atoms in the excited state are always possessing a different momentum than those in the ground state, the proccess of both transmission and reflection can be used as a device to split the atomic beam in a coherent way. These calculations can be applied to an exact description of an interferometer with stationary interaction geometry.

We assume that the periodic potential has a rectangular envelope or profile, see Fig. 1. In other words, the potential is bound by two parallel planes Σ and Σ' possessing antiparallel normals $\boldsymbol{n}$ and $\boldsymbol{n}'$ and has a constant amplitude between these two surfaces. We calculate the intensities of the transmitted and reflected beams as functions of the incoming beam.

In order to describe the beam splitters in the spatial interaction geometry, we use the stationary two-level Schrödinger equation in a rotating frame

$$E\psi(\boldsymbol{x}) = \left(\frac{\hat{\boldsymbol{p}}^2}{2m} - \frac{1}{2}\,\hbar\omega\sigma_3 + H_{\text{atom}} + H_{\text{dip}}(\boldsymbol{x})\right)\psi(\boldsymbol{x})\,. \tag{1}$$

Here σ_3 is the third Pauli matrix, and

$$H_{\text{atom}} = \begin{pmatrix} E_b & 0 \\ 0 & E_a \end{pmatrix} = \frac{1}{2}\,(E_a + E_b) + \frac{1}{2}\,\hbar\omega_{ba}\sigma_3\,, \tag{2}$$

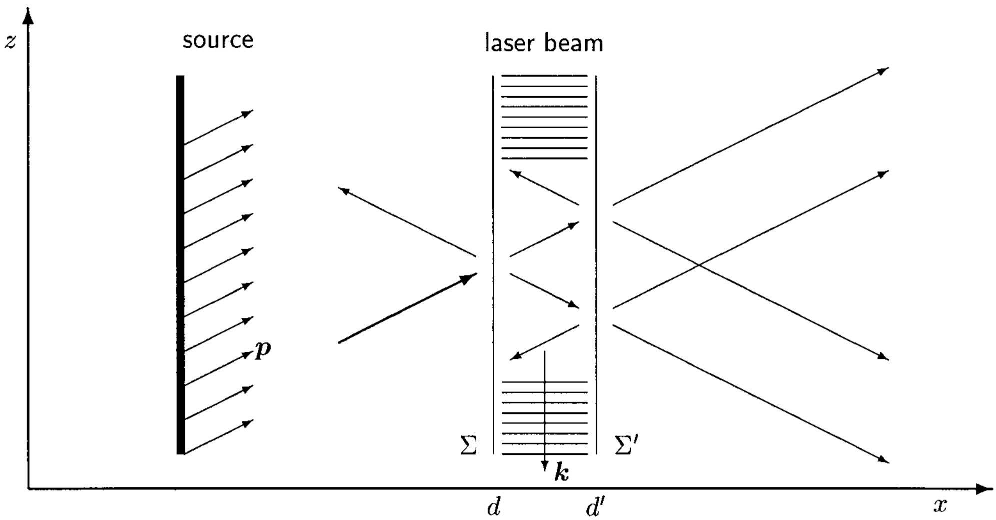

Fig. 1 Geometry of the beam splitters. Originating from a stationary source, atomic plane waves with momentum $\boldsymbol{p}$ enter the laser region between the surfaces Σ and Σ'. These surfaces are described by $x = d$ and $x = d'$, respectively, with $d' = d + l$. With a certain probability, the wave vector of the laser beam $\boldsymbol{k}$ is transferred to the atomic wave so that the transmitted wave is split into two atomic waves.

with $\omega_{ba} := (E_b - E_a)/\hbar$, and

$$H_{\text{dip}}(\boldsymbol{x}) = -\hbar\Omega_{ba} \cdot \begin{pmatrix} 0 & e^{i\boldsymbol{k}\cdot\boldsymbol{x}} \\ e^{-i\boldsymbol{k}\cdot\boldsymbol{x}} & 0 \end{pmatrix} \tag{3}$$

where E_b and E_a are the upper and lower energy levels of the atom. We denote with m the mass of the atom, and $\Omega_{ba} = \frac{1}{2\hbar} |\langle a| \mu E |b\rangle|$ is the Rabi frequency. Furthermore, ω and $\boldsymbol{k}$ are the frequency and the wave vector of the laser beam. We neglect any relaxation effects. We have already removed any time-dependence from the dipole interaction term, compare [8].

As usual, the probability current is given by

$$\boldsymbol{j} = -\frac{i\hbar}{2m}\,(\psi^+\nabla\psi - \nabla\psi^+\psi) = -\frac{\hbar}{m}\,\text{Re}(\psi^+ i\nabla\psi)\,. \tag{4}$$

We base our theory of the stationary beam splitting process on equation (1). The procedure for describing the beam splitting process is the same in principle as the calculation of the reflected and transmitted parts of an incoming plane wave hitting a potential barrier. In our case the incoming wave is represented by a two-level system and the potential barrier possesses a periodic structure, see Fig. 1. In our calculations we will not use any approximation, except when we use the 'limit of high kinetic energy' of the atoms for comparison with known results.

2 The exact solution

2.1 The wave function

We first introduce

$$\psi'_b(\boldsymbol{x}) = e^{-i\boldsymbol{k}\cdot\boldsymbol{x}}\psi_b(\boldsymbol{x})\,, \tag{5}$$

$$\psi'_a(\boldsymbol{x}) = \psi_a(\boldsymbol{x})\,, \tag{6}$$

and get from (1) two equations the coefficients of which do not depend on $\boldsymbol{x}$:

$$E'\psi'_b(\boldsymbol{x}) = \left(-\frac{\hbar^2}{2m}\,(\nabla^2 + 2i\boldsymbol{k}\cdot\nabla - k^2) - \hbar\Delta\right)\psi'_b(\boldsymbol{x}) - \hbar\Omega_{ba}\psi'_a(\boldsymbol{x})\,, \tag{7}$$

$$E'\psi'_a(\boldsymbol{x}) = -\frac{\hbar^2}{2m}\,\nabla^2\psi'_1(\boldsymbol{x}) - \hbar\Omega_{ba}\psi'_b(\boldsymbol{x})\,, \tag{8}$$

with

$$E' := E - E_a - \frac{\hbar}{2}\,\omega\,, \tag{9}$$

and the detuning $\Delta = \omega - \omega_{ba}$. We also have $E' = E - \frac{1}{2}(E_a + E_b) - \frac{\hbar}{2}\,\Delta$. We introduced E' in order to have the detuning on the right hand side. In addition, we shall see later that E' has a simple physical interpretation because it is connected with the kinetic energy of an atom in laser-free space.

Eqs. (7, 8) are a system of partial differential equations with constant coefficients which always possesses plane wave solutions. Therefore we make the ansatz

$$\psi'_b = e^{\frac{i}{\hbar}\boldsymbol{p}\cdot\boldsymbol{x}}a_b(\boldsymbol{p})\,, \tag{10}$$

$$\psi'_a = e^{\frac{i}{\hbar}\boldsymbol{p}\cdot\boldsymbol{x}}a_a(\boldsymbol{p})\,, \tag{11}$$

and look for solutions for $\boldsymbol{p}$ and a. In order to describe the action of a stationary laser beam with a rectangular profile on a stationary atomic wave function we have to solve the wave functions for the various regions and glue them together by using some jump conditions.

If we insert this ansatz into the equation for the probability density and for the current density, we get

$$\varrho = (a_b^* a_b + a_a^* a_a)\,, \tag{12}$$

$$\boldsymbol{j} = \frac{1}{m}\left((\boldsymbol{p} + \hbar\boldsymbol{k})\, a_b^* a_b + \boldsymbol{p} a_a^* a_a\right). \tag{13}$$

Note that the momenta of the excited and ground states are $(\boldsymbol{p} + \hbar\boldsymbol{k})$ and $\boldsymbol{p}$, respectively. In addition, any imaginary part of $\boldsymbol{p}$ (evanescent modes) does not contribute to the current.

The ansatz (10, 11) will be inserted into (7) and (8) and results in the two algebraic equations

$$0 = \begin{pmatrix} \frac{(\boldsymbol{p} + \hbar\boldsymbol{k})^2}{2m} - E' - \hbar\Delta & -\hbar\Omega_{ba} \\ -\hbar\Omega_{ba} & \frac{\boldsymbol{p}^2}{2m} - E' \end{pmatrix} \begin{pmatrix} a_b \\ a_a \end{pmatrix}. \tag{14}$$

In the case where the atomic Hamiltonian has additional terms $H_{\text{atom}} = \begin{pmatrix} V_{bb} & 0 \\ 0 & V_{aa} \end{pmatrix}$, this will amount to the replacements $E' \to E' - V_{aa}$ and $\hbar\Delta \to \hbar\Delta + V_{aa} - V_{bb}$.

Before discussing the dispersion relation we first display the solutions $a = \begin{pmatrix} a_b \\ a_a \end{pmatrix}$. For the state a of (10, 11) we find, after normalization $a^+(\boldsymbol{p})\, a(\boldsymbol{p}) = 1$, the two solutions[1]

$$a_{1,2}(\boldsymbol{p}) = \begin{pmatrix} \sqrt{A_{1,2}(\boldsymbol{p})} \\ \mp\sqrt{A_{2,1}(\boldsymbol{p})} \end{pmatrix} \tag{15}$$

(here the $\mp$ corresponds to 1, 2) with

$$A_{1,2}(\boldsymbol{p}) = \frac{1}{2}\left(1 \pm \frac{y(\boldsymbol{p})}{\sqrt{1 + y^2(\boldsymbol{p})}}\right) \tag{16}$$

and

$$y(\boldsymbol{p}) := \frac{1}{2\hbar\Omega_{ba}}\left(\frac{(\boldsymbol{p} + \hbar\boldsymbol{k})^2}{2m} - \frac{\boldsymbol{p}^2}{2m} - \hbar\Delta\right). \tag{17}$$

The function $y(\boldsymbol{p})$ which is characteristic for the beam splitting, is defined in analogy with the theory of dynamical diffraction of neutrons in crystals [10]. In atom optics this function contains information about the relation between the laser fre-

[1] Indices 1, 2 indicate the two energy eigenstates, and indices a, b the upper and the lower atomic level.

quency ω and the internal energy levels, and about the relation between the momentum of the atoms and the wave vector $\boldsymbol{k}$ of the laser beam. Since, contrary to neutron interferometry, ω and $\boldsymbol{k}$ are easily varied a richer variety of physical effects is expected in our case. It is clear that the function $y(\boldsymbol{p})$ depends on the tangential parts of $\boldsymbol{p}$ only because, owing to Maxwell's equations, $\boldsymbol{k}$ is orthogonal to the normal $\boldsymbol{n}$. The function $y(\boldsymbol{p})$ can be made to vanish by choosing an appropriate detuning. For zero detuning, this function is identical with the corresponding function in neutron optics where it describes the departure from the Bragg condition $p_z = -\frac{1}{2}\hbar k$. We also note that, for $\Omega_{ba} = 0$, we have $A_1 = 1$ and $A_2 = 0$ and, for $\Omega_{ba} \neq 0$, we also find $0 < A_{1,2}(\boldsymbol{p}) < 1$.

The general solution of (14), corresponding to the momenta $\boldsymbol{p}_1$ and $\boldsymbol{p}_2$ which, for a fixed energy E', are solutions of (21) and (22), is given by

$$\psi' = \alpha_1^+ \psi_1'^+ + \alpha_2^+ \psi_2'^+ + \alpha_1^- \psi_1'^- + \alpha_2^- \psi_2'^- \,, \tag{18}$$

where $\alpha_{1,2}^{\pm}$ are complex constants which have to be determined by boundary conditions, and (see Fig. 5)

$$\psi_{1,2}'^+ = e^{\frac{i}{\hbar}\boldsymbol{p}_{1,2}\cdot\boldsymbol{x}} a_{1,2}(\boldsymbol{p}) \,, \qquad \psi_{1,2}'^- = e^{\frac{i}{\hbar}\boldsymbol{p}_{1,2}^{\text{refl.}}\cdot\boldsymbol{x}} a_{1,2}(\boldsymbol{p}) \,. \tag{19}$$

2.2 The dispersion relation

The solvability condition for equation (14) requires the vanishing of the determinant of the coefficient matrix and gives a Hamilton-Jacobi equation (or dispersion relation) for the wave vector $\boldsymbol{p}$:

$$0 = \left(\frac{(\boldsymbol{p} + \hbar\boldsymbol{k})^2}{2m} - E' - \hbar\Delta\right)\left(\frac{\boldsymbol{p}^2}{2m} - E'\right) - \hbar^2\Omega_{ba}^2 \,. \tag{20}$$

In this equation E', Δ, and Ω_{ba} are given quantities. Owing to the translational symmetry of the problem along the y- and z-axes the momenta p_y and p_z are conserved quantities and can be globally prescribed. Consequently, eqn. (20) is a fourth order equation for the momentum p_x so that in general the dispersion relation consists of two disconnected components.

The structure of the Hamilton-Jacobi equation (20) is better exhibited if we solve this equation for the constant energy E'. In this case we get two Hamilton-Jacobi equations

$$E' = f_1(\boldsymbol{p}) = \frac{1}{2m}\boldsymbol{p}^2 + \hbar\Omega_{ba}\left(y(\boldsymbol{p}) + \sqrt{1 + y^2(\boldsymbol{p})}\right) \tag{21}$$

and

$$E' = f_2(\boldsymbol{p}) = \frac{1}{2m}\boldsymbol{p}^2 + \hbar\Omega_{ba}\left(y(\boldsymbol{p}) - \sqrt{1 + y^2(\boldsymbol{p})}\right), \tag{22}$$

The solvability condition now reads

$$0 = (E' - f_2(\boldsymbol{p}))(E' - f_1(\boldsymbol{p})) \,. \tag{23}$$

These two Hamilton-Jacobi equations are constraints for the momenta $\boldsymbol{p}$. If two components of $\boldsymbol{p}$ are given, the third one can be determined by means of these equations. As suggested by the symmetry of our problem, we take the components $\boldsymbol{p}_t$ tangential to the surface of the laser region as given so that, by means of the Hamilton-Jacobi equations, we can calculate the normal part p_n of the momentum. Then (21) and (22) reduce to equations of the simple form $E'' = p_n^2/2m$ which can easily be solved for p_n.

The relations (21) and (22) yield as usual the interpretation of the energy eigenvalue E' for the stationary Schrödinger equation: E' consists of the kinetic energy and additional terms depending on the Doppler-term $\boldsymbol{p} \cdot \boldsymbol{k}$ and on the detuning Δ. All these laser-related terms contribute to the energy of the two-level atom.

Therefore we have four independent states with four different momenta, see Fig. 2, 3, and 4. The four independent states are states with the same energy but with different wave vectors. The explicit solutions of the Hamilton-Jacobi equations (21) and (22) are given by $p_n = \pm p_{n,1,2}$,

$$p_{n,1,2} = \sqrt{2m}\left(E' - E^{\perp}_{\text{kin}} - \hbar\Omega_{ba}\left(y(\boldsymbol{p}) \mp \sqrt{1 + y^2(\boldsymbol{p})}\right)\right)^{\frac{1}{2}}, \tag{24}$$

with $E^t_{\text{kin}} := \frac{1}{2m}\,\boldsymbol{p}_t^2$. The indices $1, 2$ in the solution (24) are related to the two-level structure of the quantum system. We also have

$$p_{n,2} = \sqrt{p_{n,1}^2 - 4m\hbar\Omega_{ba}\sqrt{1 + y^2(\boldsymbol{p})}}\;. \tag{25}$$

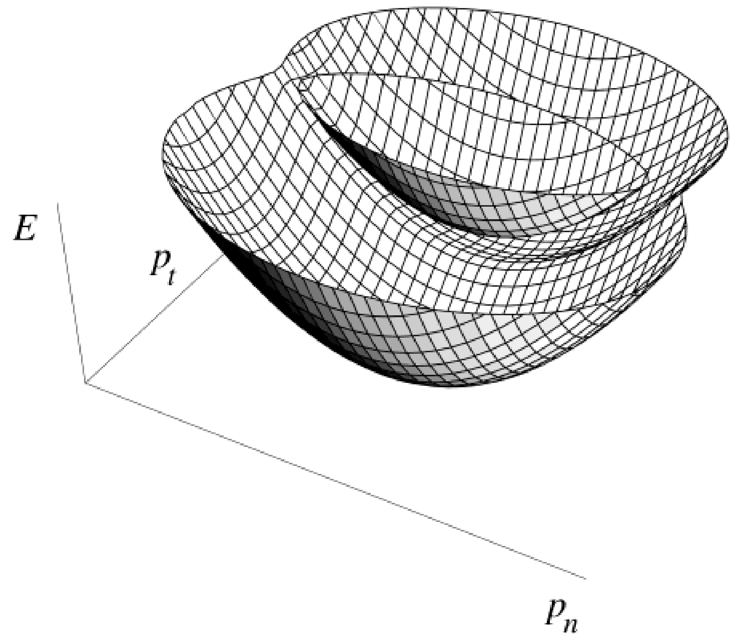

Fig. 2 The dispersion relation (20) for $\Omega_{ba} \neq 0$. The energy E is a function of the normal and tangential components p_n, $\boldsymbol{p}_t$ of the momentum. In our example we use $\hbar k = 10$, $\hbar\Omega_{ba} = 10$ and $\Delta = 20$ in arbitrary units.

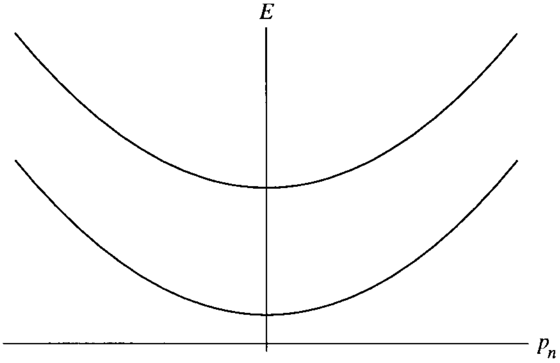

Fig. 3 The energy E as a function of the normal component of the momentum p_n, the tangential part $\boldsymbol{p}_t$ is constant.

The two components of the dispersion relation, generally disconnected, and the corresponding solutions for the momentum are called in the case of neutron diffraction by Werner [11] 'branch α' and 'branch β'.

Let us further explain the physics inside the laser beam by using the dispersion relation (20) or the two corresponding relations (21) and (22). First we plot the dispersion surface $E' = E'(p_n, \boldsymbol{p}_t)$. In general we get two disconnected surfaces, see Fig. 2.

In the case of fixed $\boldsymbol{p}_t$ we get the energy E' as function of the momentum p_n (in our approach E' is of course prescribed and p_n is calculated), see Fig. 3. The slope $\partial E'/\partial p_n$ yields the group velocity in direction of the surface, that is, parallel to the normal $\boldsymbol{n}$.

Fig. 4 represents a cut along a line orthogonal to the p_n axis. The smallest distance between these two curves is given by the Rabi frequency $\hbar\Omega_{ba}$. In the case of vanishing laser beam this diagram consists of two parabolae which are translated in tangential direction by $\hbar k$ and on the energy axis by $\hbar\Delta$.

From this figure, we can learn that there is a splitting of the tangential part of the group velocity of the atomic beam while the tangential part of the momentum $\boldsymbol{p}_t$ is fixed and continuous. The group velocity is given by the gradient

$$\boldsymbol{v} := \nabla_{\boldsymbol{p}} E(\boldsymbol{p})\,. \tag{26}$$

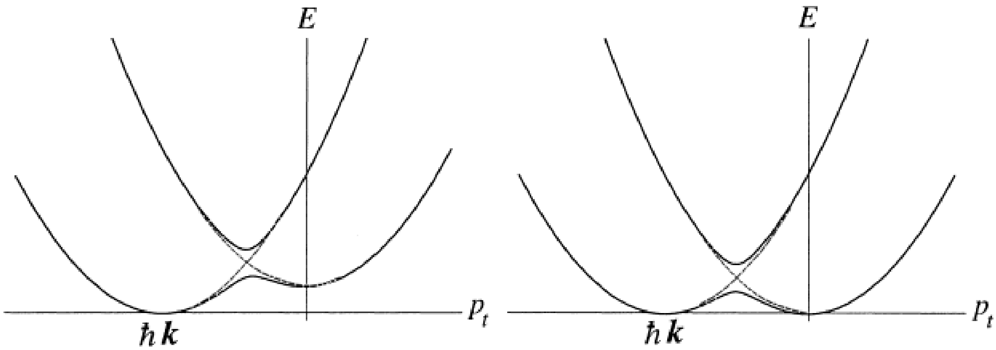

Fig. 4 The energy E as a function of the tangential part $\boldsymbol{p}_t$ of the momentum. The right figure is for $y = 0$. The gray lines are the corresponding diagrams for vanishing laser beam, $\Omega_{ba} = 0$. The normal part p_n is taken to be constant. The two minima are horizontally separated by $\hbar\boldsymbol{k}$ and vertically by y. The Rabi frequency $\hbar\Omega_{ba}$ determines the spacing between both curves.

Using the two expressions for the energy (21) and (22) we get

$$\boldsymbol{v}_{1,2} = \nabla_{\boldsymbol{p}} f_{1,2}(\boldsymbol{p})\big|_{\boldsymbol{p}_{1,2}} = \frac{\boldsymbol{p}_{1,2}}{m} + A_{1,2}(\boldsymbol{p})\,\frac{\hbar \boldsymbol{k}}{m}\,. \tag{27}$$

From this result and by inspection of Fig. 4 it is clear that, in general, the group velocity is not proportional to the momentum. For the z-component of the group velocity, which is relevant for the splitting of the atomic beams, we get

$$v_{z,1,2} = \frac{p_z}{m} + A_{1,2}(\boldsymbol{p})\,\frac{\hbar k}{m}\,. \tag{28}$$

Especially, for $y = 0$, there is no splitting of the group velocities. If, furthermore, the detuning Δ vanishes, then this corresponds to the Bragg condition $p_z = -\frac{1}{2}\,\hbar k$, as in neutron optics.

The splitting of the two beams inside the laser region is given by

$$\delta v_z = v_{z,1} - v_{z,2} = \frac{y}{\sqrt{1+y^2}}\,\frac{\hbar k}{m}\,. \tag{29}$$

It should be noted that the direction of the splitting of the atomic beam after leaving the laser region is not affected by the splitting inside the laser region. However, these consideration may be important for a correct analysis of phase shifts of atomic interferometry experiments in external fields because in a quasiclassical treatment these phase shifts depend on the area circumvented by the atomic beams. This point has been important for neutron interferometry in gravitational fields, see [12, 13, 14] and should be important for atomic interferometry in the future.

We show in the Appendix that the group velocity is proportional to the total atomic current. Note that the group velocities $\boldsymbol{v}_{1,2}$ are *not* the velocities of the atoms in the ground state or excited state, respectively. These group velocities correspond to the two independent solutions for fixed energy.

Another feature can also be read off from Fig. 4: Since for particles described by a wave equation the inverse of the effective mass is given by the second derivative of the energy with respect to the momentum, the zz–component of the tensor of the effective mass is of opposite sign for a certain range of momenta, as can be seen in Fig. 4. Therefore we can already conclude at this stage that for a specified force the acceleration of two packets which are made of plane waves of each branch only, are in opposite directions. Indeed, these anomalous effects play a role in the beam splitting process in neutron interferometry [14] and also in atom optics as we shall see in a forthcoming article [15].

The last figure is a cut through the 3-dimensional plot for a $E' = \text{const.}$, see Fig. 5. This represents all solutions for fixed energy and thus corresponds exactly to the stationary case under consideration.

Note that the momentum in direction of the normal in general depends, via y, on the detuning Δ. Such an effect is not possible in neutron optics in crystals what establishes the superior variability of atom optics using laser beams as optical elements.

For $\Omega_{ba} = 0$, we get $p_{n,1} = p_{n,2} = \sqrt{2m}\,\sqrt{E' - E^t_{\text{kin}}}$. For $\Omega_{ba} \neq 0$, the value of $|p_{n,2}|$ will decrease so that the laser beams acts as potential barrier with an effec-

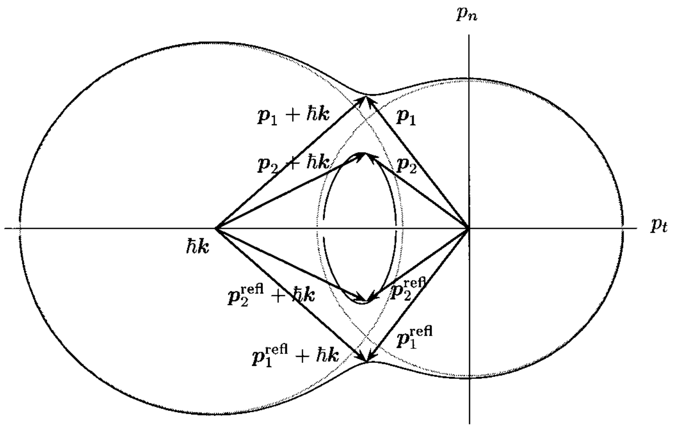

Fig. 5 The dispersion relation for $E = \text{const}$ for non–vanishing (black) and for vanishing (grey) Rabi frequency Ω_{ba}. For a given tangential part of the momentum $\boldsymbol{p}_t$ there are eight solutions for the momentum, namely $\boldsymbol{p}_1$, $\boldsymbol{p}_2$, $\boldsymbol{p}_1 + \hbar\boldsymbol{k}$, and $\boldsymbol{p}_2 + \hbar\boldsymbol{k}$ and the corresponding reflected beams $\boldsymbol{p}_1^{\rm refl}$, $\boldsymbol{p}_2^{\rm refl}$, $\boldsymbol{p}_1^{\rm refl} + \hbar\boldsymbol{k}$, and $\boldsymbol{p}_2^{\rm refl} + \hbar\boldsymbol{k}$ with $\boldsymbol{p}_1^{\rm refl} = \boldsymbol{p}_t - p_{n,1}\boldsymbol{n}$ and $\boldsymbol{p}_2^{\rm refl} = \boldsymbol{p}_t - p_{n,,2}\boldsymbol{n}$.

tive potential $V > 0$. On the other hand, $|p_{n,1}|$ will increase so that the laser region acts as a potential pot with a potential $V < 0$. In other words: one energy eigenstate feels the laser as a potential barrier, the other eigenstate as potential pot. In addition, in $p_{n,1}$ the factor connected with Ω_{ba} is always larger than zero. Consequently, for all $E' - E^t_{\rm kin} > 0$ the quantity under the square root is always positive so that $p_{n,2}$ is real. It should be noted that, due to the fact that the laser frequency can be arbitrarily chosen, the energy E is not bounded from below.

Note that the whole discussion of the dispersion surface applies to the stationary interaction geometry as well as to the beam splitters using laser pulses, provided that inside the laser region or during the laser pulses the dipole interaction is constant. The reason for that is that one first determines the solution with laser and without laser, respectively, and then glues them together using jump conditions which are given by the order of the corresponding differential equation. In the stationary case we have a differential equation of second order so that the wave function and its first derivative have to be continuous, in the pulsed case we have a first order equation only so that only the wave function must be continuous. In the latter case this leads to a simple successive application of the time evolution operator. In the following we are discussing the first case.

2.3 Vanishing laser field

In the case of a vanishing laser field, $\Omega_{ba} = 0$, we get, instead of (21, 22),

$$E' = f_{2,1}(\boldsymbol{p}_0) = \begin{cases} \dfrac{(\boldsymbol{p}_2^0 + \hbar\boldsymbol{k})^2}{2m} - \hbar\Delta\,, \\ \dfrac{(\boldsymbol{p}_1^0)^2}{2m}\,. \end{cases} \tag{30}$$

In this case we denote the momentum by $\boldsymbol{p}^0$. Therefore the energy E' can be interpreted as the total kinetic energy of a ground state atom in the laser-free space. In a momentum-energy diagram the momenta give two displaced parabolae. The minima of these parabolae are displaced in E-direction by the amount of $\hbar\Delta$ and in $\boldsymbol{p}^0$-direction by $\hbar\boldsymbol{k}$. We find the two momenta

$$p^0_{n,2} = \sqrt{2m}\,(E' - E^t_{\text{kin}} - 2\hbar\Omega_{ba}y(\boldsymbol{p}^0))^{\frac{1}{2}}\,,$$
$$p^0_{n,1} = \sqrt{2m}\,(E' - E^t_{\text{kin}})^{\frac{1}{2}}\,, \tag{31}$$

which are related by

$$p^0_{n,2} = \sqrt{(p^0_{n1})^2 - 4m\hbar\Omega_{ba}y(\boldsymbol{p}^0)}\,. \tag{32}$$

Even in free space it is necessary to consider two different $p^0_{n1,2}$ in order to get the same energy E' for both equations (7) and (8). Because y can be negative, $p^0_{n,1}$ can be larger as well as smaller than $p^0_{n,2}$. Only in the case $\frac{\hbar}{m}\,\boldsymbol{p}^0\cdot\boldsymbol{k} + \frac{\hbar k^2}{2m} = \hbar\Delta$ (Doppler shift, recoil, and detuning cancel each other) both momenta coincide. We have for the states

$$\psi_2^+ = \begin{pmatrix}1\\0\end{pmatrix} e^{i\left(\frac{1}{\hbar}\boldsymbol{p}_2^0 + \boldsymbol{k}\right)\cdot\boldsymbol{x}}\,, \qquad \psi_2^- = \begin{pmatrix}1\\0\end{pmatrix} e^{i\left(\frac{1}{\hbar}\,(\boldsymbol{p}_2^{0,\text{refl.}}\cdot\boldsymbol{k})\cdot\boldsymbol{x}\right)}\,, \tag{33}$$

$$\psi_1^+ = \begin{pmatrix}0\\1\end{pmatrix} e^{\pm\frac{i}{\hbar}\boldsymbol{p}_1^0\cdot\boldsymbol{x}}\,, \qquad \psi_1^- = \begin{pmatrix}0\\1\end{pmatrix} e^{\frac{i}{\hbar}\boldsymbol{p}_1^{0,\text{refl.}}\cdot\boldsymbol{x}}\,. \tag{34}$$

Thus, for the unprimed state $\psi = \psi_1 + \psi_2$ the excited state has total momenta $\boldsymbol{p}_2^0 + \hbar\boldsymbol{k}$ and $\boldsymbol{p}_2^{0,\text{refl.}} + \hbar\boldsymbol{k}$ and the lower state momenta $\boldsymbol{p}_1^{0,\text{refl.}}$ and $\boldsymbol{p}_1^{0,\text{refl.}}$. Although allowed by energy conservation, there is no excited state possessing momenta $\boldsymbol{p}_2^0$ or $p_2^{0,\text{refl.}}$ and no ground state with momenta $\boldsymbol{p}_1^0 + \hbar\boldsymbol{k}$ or $\boldsymbol{p}_1^{0,\text{refl.}} + \hbar\boldsymbol{k}$.

3 Entering the laser region

Before describing the beam splitting of an atomic beam by travelling through a laser region, we first discuss what happens with the atomic beam while entering the laser region.

3.1 Matching the momenta

Since the tangential part of $\boldsymbol{p}$ is prescribed, only the normal part of $\boldsymbol{p}$ can change by entering the laser region. In addition, according to general principles of quantum mechanics, the wave function as well as its first derivative are continuous at the boundary of the laser region. The atomic beam in the laser region is given by plane waves $\exp\left(\frac{i}{\hbar}\,\boldsymbol{p}_{1,2}\cdot\boldsymbol{x}\right)$ and $\exp\left(\frac{i}{\hbar}\,\boldsymbol{p}_{1,2}^{\text{refl.}}\cdot\boldsymbol{x}\right)$ and in the laser-free region by $\exp\left(\frac{i}{\hbar}\,\boldsymbol{p}^0_{1,2}\cdot\boldsymbol{x}\right)$ and $\exp\left(\frac{i}{\hbar}\,\boldsymbol{p}^{0\,\text{refl.}}_{1,2}\cdot\boldsymbol{x}\right)$. Therefore the plane waves are $\exp\left(\frac{i}{\hbar}\,(\pm p_{n1,2}x_n + \boldsymbol{p}_t\cdot\boldsymbol{x})\right)$, where $\boldsymbol{p}_t = \boldsymbol{p}_{1t} = \boldsymbol{p}_{2t} = \boldsymbol{p}^0_{1t} = \boldsymbol{p}^0_{2t}$ is the same prescribed momentum inside and outside the laser region.

From the globally constant energy, we can express the momentum inside the laser region as function of the momentum in free space. In case that the atomic beam outside is in an excited state, we have the condition

$$\frac{\boldsymbol{p}^2}{2m} + \hbar\Omega_{ba}\left(y(\boldsymbol{p}) \pm \sqrt{1 + y^2(\boldsymbol{p})}\right) = \frac{(\boldsymbol{p}_2^0 + \hbar\boldsymbol{k})^2}{2m} - \hbar\Delta\,, \tag{35}$$

and if the atom outside is in the ground state,

$$\frac{\boldsymbol{p}^2}{2m} + \hbar\Omega_{ba}\Big(y(\boldsymbol{p}) \pm \sqrt{1 + y^2(\boldsymbol{p})}\Big) = \frac{(\boldsymbol{p}_2^0)^2}{2m} \,. \tag{36}$$

We split the momentum into tangential and normal components and solve the resulting equations for the normal part inside the laser region (note that the function y depends on $\boldsymbol{p}_t$ only which is the same outside and inside the laser region),

$$p_{n,1,2} = \sqrt{(p_{n,1}^0)^2 - 2m\hbar\Omega_{ba}\Big(y(\boldsymbol{p}) \mp \sqrt{1 + y^2(\boldsymbol{p})}\Big)} \tag{37}$$

and in case, the outside atom is in the excited state,

$$p_{n,1,2} = \sqrt{(p_{n,2}^0)^2 + 2m\hbar\Omega_{ba}\Big(y(\boldsymbol{p}) \pm \sqrt{1 + y^2(\boldsymbol{p})}\Big)} \tag{38}$$

In (37) the momenta inside the laser region are expressed in terms of the momentum of the ground state atom while in (38) it is expressed as function of the momenta of atoms in the excited state. Using the relation between the momenta of the excited and ground state atom in free space, both expressions prove to be identical. Each of these results describes that all four momenta $\pm p_{n,1,2}$ are excited if an atomic beam enters the laser region, irrespective of the internal state of the entering atom.

In terms of the unprimed wavefunction, inside the laser region, we have eight waves with momenta $\boldsymbol{p}_1$, $\boldsymbol{p}_2$, $\boldsymbol{p}_1 + \hbar\boldsymbol{k}$, $\boldsymbol{p}_2 + \hbar\boldsymbol{k}$, $\boldsymbol{p}_1^{\text{refl.}}$, $\boldsymbol{p}_2^{\text{refl.}}$, $\boldsymbol{p}_1^{\text{refl.}} + \hbar\boldsymbol{k}$, and $\boldsymbol{p}_2^{\text{refl.}} + \hbar\boldsymbol{k}$.

3.2 Matching the amplitudes

The complete description of the situation is given by

$$\psi' = \begin{cases} A_2\begin{pmatrix}1\\0\end{pmatrix} e^{i\boldsymbol{p}_2^0\cdot\boldsymbol{x}} + A_1\begin{pmatrix}0\\1\end{pmatrix} e^{i\boldsymbol{p}_1^0\cdot\boldsymbol{x}} + B_2\begin{pmatrix}1\\0\end{pmatrix} e^{-i\boldsymbol{p}_2^{0,\text{refl.}}\cdot\boldsymbol{x}} + B_1\begin{pmatrix}0\\1\end{pmatrix} e^{-i\boldsymbol{p}_1^{0,\text{refl.}}\cdot\boldsymbol{x}} & \text{for } x < d \\ C_2\begin{pmatrix}\sqrt{A_+(p)}\\ -\sqrt{A_-(p)}\end{pmatrix} e^{i\boldsymbol{p}_2\cdot\boldsymbol{x}} + C_1\begin{pmatrix}\sqrt{A_-(p)}\\ \sqrt{A_+(p)}\end{pmatrix} e^{i\boldsymbol{p}_1\cdot\boldsymbol{x}} & \\ \qquad + D_2\begin{pmatrix}\sqrt{A_+(p)}\\ -\sqrt{A_-(p)}\end{pmatrix} e^{-i\boldsymbol{p}_2^{\text{refl.}}\cdot\boldsymbol{x}} + D_1\begin{pmatrix}\sqrt{A_-(p)}\\ \sqrt{A_+(p)}\end{pmatrix} e^{-i\boldsymbol{p}_1^{\text{refl.}}\cdot\boldsymbol{x}} & \text{for } d < x \end{cases} \tag{39}$$

The boundary conditions state that ψ' as well as its derivative has to be continuous at $x = d$: Therefore $(\psi(d\pm) := \lim_{\epsilon\to 0}\psi(d \pm \epsilon))$

$$\psi(d-) = \psi(d+), \qquad \frac{\partial}{\partial x}\,\psi(d-) = \frac{\partial}{\partial x}\,\psi(d+) \,. \tag{40}$$

By equating the wave functions for the dark zone and the laser zone, the exponential belonging to the prescribed momenta $\exp\left(\frac{i}{\hbar}\,\boldsymbol{p}_t\cdot\boldsymbol{x}\right)$ drop out.

The conditions above yield four equations relating $C_{1,2}$ and $D_{1,2}$ to $A_{1,2}$ and $B_{1,2}$. We define

$$\mathcal{A} = \begin{pmatrix}A_2\\A_1\end{pmatrix}, \qquad \mathcal{B} = \begin{pmatrix}B_2\\B_1\end{pmatrix}, \qquad \mathcal{C} = \begin{pmatrix}C_2\\C_1\end{pmatrix}, \qquad \mathcal{D} = \begin{pmatrix}D_2\\D_1\end{pmatrix}, \tag{41}$$

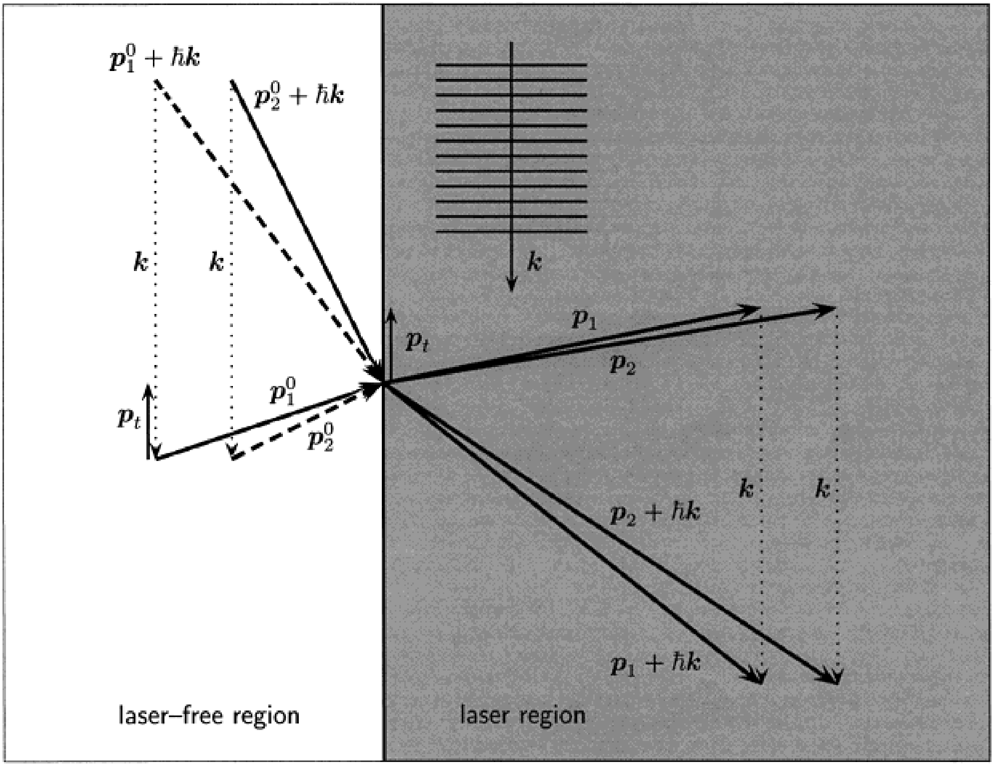

Fig. 6 Visualisation of the momenta of the atomic waves before and after entering the laser region. Taking into account the addition of the wave vector of the laser beam, in laser–free space there are four possible momenta of the atoms: $\boldsymbol{p}_{1,2}^0$ and $\boldsymbol{p}_{1,2}^0 + \hbar\boldsymbol{k}$. According to (33, 34), the two incoming momenta $\boldsymbol{p}_1^0 + \hbar\boldsymbol{k}$ and $\boldsymbol{p}_2^0$ (dashed vectors) are in fact not present (although allowed by energy conservation) because the corresponding amplitudes vanish. It should be kept in mind that the figure above represents position space only in the sense that the momenta are restricted to the regions before and behind the boundary of the laser region.

and get from (40)

$$\mathbb{M}_d^{(0)} \begin{pmatrix} \mathcal{A} \\ \mathcal{B} \end{pmatrix} = \mathbb{M}_d \begin{pmatrix} \mathcal{C} \\ \mathcal{D} \end{pmatrix}, \tag{42}$$

with

$$\mathbb{M}_d = \begin{pmatrix} \sqrt{A_+} e^{ip_2 d} & \sqrt{A_-} e^{ip_1 d} & \sqrt{A_+} e^{-ip_2 d} & \sqrt{A_-} e^{-ip_1 d} \\ -\sqrt{A_-} e^{ip_2 d} & \sqrt{A_+} e^{ip_1 d} & -\sqrt{A_-} e^{-ip_2 d} & \sqrt{A_+} e^{-ip_1 d} \\ \sqrt{A_+} p_{n2} e^{ip_2 d} & \sqrt{A_-} p_{n1} e^{ip_1 d} & -\sqrt{A_+} p_{n2} e^{-ip_2 d} & -\sqrt{A_-} p_{n1} e^{-ip_1 d} \\ -\sqrt{A_-} p_{n2} e^{ip_2 d} & \sqrt{A_+} p_{n1} e^{ip_1 d} & \sqrt{A_-} p_{n2} e^{-ip_2 d} & -\sqrt{A_+} p_{n1} e^{-ip_1 d} \end{pmatrix} \tag{43}$$

and $\mathbb{M}_d^0 = \mathbb{M}_d(\Omega_{ba} = 0)$. (Here and in the following we denote for simplicity $p_{1,2} = p_{n,1,2}$ and $p_{1,2}^0 = p_{n,1,2}^0$.) Eqn. (42) relates the coefficients of the atomic beam in front of the laser region to that behind the entrance surface. If we treat the problem of an infinitely large laser region ($\Omega_{ba} \neq 0$ for $x \geq 0$), then we can take as boundary condition $D_1 = D_2 = 0$ and can solve C_1, C_2 in terms of the incoming A_1, A_2 (see below).

3.3 The Borrmann effect

The Borrmann effect is known from dynamical neutron diffraction. It describes the phenomenon that, only for a certain angle of the incident momentum with the surface of the crystal, the propagation of the neutrons inside the crystal is normal to the surface, see Fig. 7. In addition, only if this is the case there will be no attenuation of the neutron beam inside the crystal due to interactions with the atomic cores. A similar phenomenon occurs in our case of atoms entering a laser region. However, the physics is different and there is also no attenuation of the atoms because they cannot be absorbed by the laser beams.

We first calculate the tangential component of the current inside the laser region as function of the parameters of the atomic beam entering the laser region. We treat the problem for a laser region which covers the whole half space $x \geq 0$. In this case there are no waves running back, that is, $D_1 = D_2 = 0$ in (39).

The current inside the laser region is

$$\boldsymbol{j} = -\frac{i\hbar}{2m}\left(\psi^{+}\nabla\psi - \nabla\psi^{+}\psi\right) = \boldsymbol{j}_a + \boldsymbol{j}_b = \boldsymbol{j}_1 + \boldsymbol{j}_2\,, \tag{44}$$

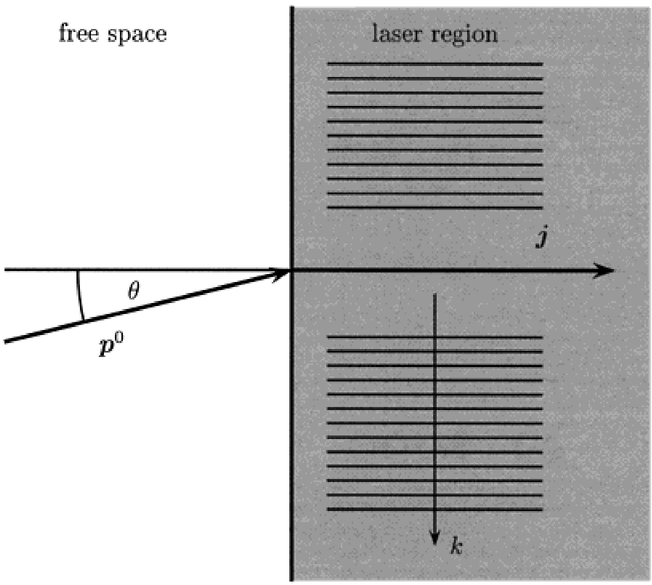

Fig. 7 The Borrmann effect for the total current: If the momentum $\boldsymbol{p}^0$ of the incoming atomic beam has a specific angle θ_{Bragg} with the normal of the surface of the laser region, then the averaged total current $\langle \boldsymbol{j} \rangle$ of the atomic beam inside the laser region is proportional to this normal. In the case of neutron diffraction, the role of $\boldsymbol{k}$ is taken over by the reciprocal lattice vector near the Ewald sphere specified by the momentum of the incoming neutron.

with

$$\boldsymbol{j}_a = \frac{\boldsymbol{p}}{m}\,\varrho_a\,, \qquad \boldsymbol{j}_b = \frac{1}{m}\,(\boldsymbol{p} + \hbar\boldsymbol{k})\,\varrho_b \tag{45}$$

$$\boldsymbol{j}_1 = -\frac{i\hbar}{2m}\,(\psi_1^+\nabla\psi_1 - \nabla\psi_1^+\psi_1), \qquad \boldsymbol{j}_2 = -\frac{i\hbar}{2m}\,(\psi_2^+\nabla\psi_2 - \nabla\psi_2^+\psi_2) \tag{46}$$

where

$$\begin{aligned}\varrho_b &= \psi_b^*\psi_b \\ &= |C_2|^2\,A_+ + |C_1|^2\,A_- + 2\,\sqrt{A_+A_-}\;\mathrm{Re}\,(C_1^*C_2e^{i(\boldsymbol{p}_1-\boldsymbol{p}_2)\cdot\boldsymbol{x}})\,,\end{aligned} \tag{47}$$

$$\begin{aligned}\varrho_a &= \psi_a^*\psi_a \\ &= |C_2|^2\,A_- + |C_1|^2\,A_+ - 2\,\sqrt{A_+A_-}\;\mathrm{Re}\,(C_2^*C_1e^{i(\boldsymbol{p}_1-\boldsymbol{p}_2)\cdot\boldsymbol{x}})\,,\end{aligned} \tag{48}$$

where ψ is inserted from (39). The coefficients C_1 and C_2 have to be calculated, according to (45), with $D_1 = D_2 = 0$. We get

$$C_2 = \frac{1}{W}\,c_2\,, \qquad c_2 = A_2\,\sqrt{A_+}\,p_2^0(p_1^0 + p_1) - A_1\,\sqrt{A_-}\,p_1^0(p_2^0 + p_1)\,, \tag{49}$$

$$C_1 = \frac{1}{W}\,c_1\,, \qquad c_1 = A_2\,\sqrt{A_-}\,p_2^0(p_1^0 + p_2) + A_1\,\sqrt{A_+}\,p_1^0(p_2^0 + p_2)\,, \tag{50}$$

with

$$W = \frac{1}{2}\,\left(A_-(p_2^0 + p_1)\,(p_1^0 + p_2) + A_+(p_1^0 + p_1)\,(p_2^0 + p_2)\right). \tag{51}$$

This yields

$$\varrho_b = \frac{1}{W^2}\,\left(|c_2|^2\,A_+ + |c_1|^2\,A_- + 2\,\sqrt{A_+A_-}\;\mathrm{Re}\,(c_1^*c_2e^{\frac{i}{\hbar}(\boldsymbol{p}_1-\boldsymbol{p}_2)\cdot\boldsymbol{p}})\right), \tag{52}$$

$$\varrho_a = \frac{1}{W^2}\,\left(|c_2|^2\,A_- + |c_1|^2\,A_+ - 2\,\sqrt{A_+A_-}\;\mathrm{Re}\,(c_2^*c_1e^{\frac{i}{\hbar}(\boldsymbol{p}_1-\boldsymbol{p}_2)\cdot\boldsymbol{x}})\right). \tag{53}$$

There are now three distinguished effects, all of them are related to the Borrmann effect. The first case describes the effect that, for a certain momentum of the incoming atomic beam, the total current lies in direction of the normal, $\langle j_z\rangle = 0$, where $\langle\cdot\rangle$ means the average over distances larger than $\hbar/(p_1 - p_2)$. The second case describes more specifically that the average of both currents belonging to the atoms in the excited as well as in the ground state, are parallel to the normal, $\langle j_{z,a}\rangle = 0$ and $\langle j_{z,b}\rangle = 0$, and the third case requires the same for the two currents $\boldsymbol{j}_1$ and $\boldsymbol{j}_2$ or group velocities $\boldsymbol{v}_1$ and $\boldsymbol{v}_2$ connected with the two independent solutions for a given energy. We discuss all three cases:

1. The first condition is fulfilled if

$$p_z = -\frac{\langle\varrho_b\rangle}{\langle\varrho_a\rangle + \langle\varrho_b\rangle}\;\hbar k\,. \tag{54}$$

Consequently, from (52) and (53),

$$p_z = -\frac{|c_2|^2\,A_+ + |c_1|^2\,A_-}{|c_1|^2 + |c_2|^2}\;\hbar k\,, \tag{55}$$

where we can express the momenta p_2^0, p_2, and p_1 in terms of p_1^0, Ω_{ba}, y, and, of course, the parameters A_1 and A_2 describing the incoming atom beam. Eqn. (55) is the exact condition for this Borrmann effect.

We now discuss the case when the incoming atom is in the ground state: $A_2 = 0$, $A_1 = 1$. Then

$$p_z = -A_+A_- \frac{(p_2^0 + p_1)^2 + (p_2^0 + p_2)^2}{A_+(p_2^0 + p_2)^2 + A_-(p_2^0 + p_1)^2} \hbar k \,. \tag{56}$$

If the incoming atom is in the excited state, $A_2 = 1$, $A_1 = 0$, then we get

$$p_z + \hbar k = \left(1 - \frac{A_+^2(p_1^0 + p_1)^2 + A_-^2(p_1^0 + p_2)^2}{A_-(p_1^0 + p_2)^2 + A_+(p_1^0 + p_1)^2}\right) \hbar k \,. \tag{57}$$

Note that the total momentum of the incoming atom in the excited state is $\boldsymbol{p} + \hbar \boldsymbol{k}$.

We consider the angle between the momentum of the incoming atomic beam and the surface of the laser region. In the first case this angle is $\cos\theta = p_z/|p_1^0|$, and in the second case $\cos\theta = (p_z + \hbar k)/|\boldsymbol{p}_2^0 + \hbar \boldsymbol{k}|$ and is thus different from the first case. The difference vanishes for vanishing laser field ($\Omega_{ba} \to 0$), see also the approximation in Sec. 5.1.

2. For the second case (Fig. 8 (left)) we have the conditions

$$\langle \varrho_a \rangle = 0 \quad \text{and} \quad \langle \varrho_b \rangle = 0 \,, \tag{58}$$

or

$$|c_2|^2 A_- + |c_1|^2 A_+ = 0 \quad \text{and} \quad |c_2|^2 A_+ + |c_1|^2 A_- = 0 \,. \tag{59}$$

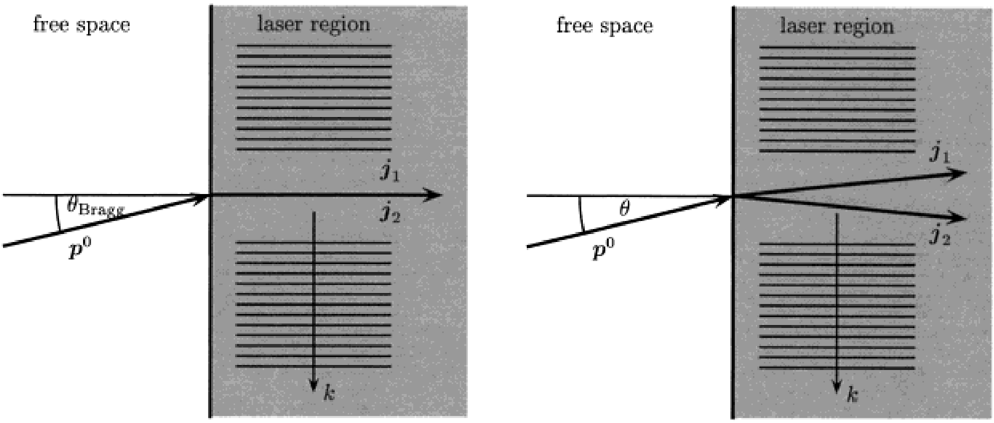

Fig. 8 The Borrmann effect for both atomic beams inside the laser region: If the momentum $\boldsymbol{p}^0$ of the incoming atomic beam has a specific angle $\theta_{\rm Bragg}$ with the normal of the surface of the laser region, then both atomic currents inside the laser region are proportional to this normal (left). This happens only for $y = 0$. In the case $y \neq 0$ both atomic currents have tangential components (right).

If the incoming atoms are in the ground state, we get

$$A_-^2 (p_2^0 + p_1)^2 + A_+^2 (p_2^0 + p_2)^2 = 0 \quad \text{and} \quad (p_2^0 + p_1)^2 + (p_2^0 + p_2)^2 = 0\,, \tag{60}$$

that is,

$$A_-^2 - A_+^2 = 0 \tag{61}$$

which is fulfilled only for $y = 0$, that is, in resonance. This means for the tangential part of the momentum of the incoming ground state atom $\boldsymbol{p} \cdot \boldsymbol{k} = m\Delta - \frac{1}{2}\,\hbar k^2$. This leads to an angle given by $\tan\theta = \left(m\Delta/k - \frac{1}{2}\hbar k\right)/p_n^0$. In the case of vanishing detuning $\Delta = 0$ we have the result $p_z = -\frac{1}{2}\,\hbar k$ known from neutron optics. If the laser is off resonance both currents $\langle \boldsymbol{j}_a \rangle$ and $\langle \boldsymbol{j}_b \rangle$ are different and not normal to the surface of the laser region, see Fig. 8 (right).

If the incoming atoms are in the excited state, we get

$$(p_1^0 + p_1)^2 + (p_1^0 + p_2)^2 = 0 \quad \text{and} \quad A_+^2 (p_1^0 + p_1)^2 + A_-^2 (p_1^0 + p_2)^2 = 0\,, \tag{62}$$

that is,

$$A_+^2 - A_-^2 = 0 \tag{63}$$

which is the same condition as above, leading to $y = 0$.

3. The last case requires that both currents $\boldsymbol{j}_1$ and $\boldsymbol{j}_2$ or group velocities $\boldsymbol{v}_1$ and $\boldsymbol{v}_2$ corresponding to the two independent solutions for fixed energy, are parallel to the normal. This means $v_{z,1} = v_{z,2} = 0$, or

$$0 = p_z + A_1(\boldsymbol{p})\,\hbar k \quad \text{and} \quad 0 = p_z + A_2(\boldsymbol{p})\,\hbar k\,. \tag{64}$$

These two equations can only be fulfilled if $y = 0$ and $p_z = -\frac{1}{2}\,\hbar k$. The corresponding incidence angle is the Bragg angle and is given by $\tan\theta_{\text{Bragg}} = -\frac{1}{2}\,\hbar k/p_n^0$. The dispersion relation for this case is displayed in the right diagram of Fig. 4.

3.4 The pendellösung

According to (49) and (51) the intensities of the atoms in the excited state and in the ground state will oscillate with the distance they move in the laser region. These oscillations are the *pendellösung* effect. The corresponding wavelength is

$$\lambda_{\text{Pendel}} = 2\pi\,\frac{\hbar}{p_1 - p_2}\,. \tag{65}$$

This *pendellösung*, as introduced for neutron optics, corresponds to the usual Rabi oscillations in atomic physics.

4 The beam splitting

Let us now treat the transmission and reflection of an atomic beam interacting with a laser region of finite width l, see Fig. 1.

4.1 Transmission and reflection matrices

For the full beam splitting process, that is, for the transition through a laser region, we have the following situation:

$$\psi' = \begin{cases} A_2\begin{pmatrix}1\\0\end{pmatrix} e^{i\boldsymbol{p}_2^0\cdot\boldsymbol{x}} + A_1\begin{pmatrix}0\\1\end{pmatrix} e^{i\boldsymbol{p}_1^0\cdot\boldsymbol{x}} + B_2\begin{pmatrix}1\\0\end{pmatrix} e^{-i\boldsymbol{p}_2^{0,\text{refl.}}\cdot\boldsymbol{x}} + B_1\begin{pmatrix}0\\1\end{pmatrix} e^{-i\boldsymbol{p}_1^{0,\text{refl.}}\cdot\boldsymbol{x}} & \text{for } x < d\,, \\ C_2\begin{pmatrix}\sqrt{A_+(p)}\\ -\sqrt{A_-(p)}\end{pmatrix} e^{i\boldsymbol{p}_2\cdot\boldsymbol{x}} + C_1\begin{pmatrix}\sqrt{A_-(p)}\\ \sqrt{A_+(p)}\end{pmatrix} e^{i\boldsymbol{p}_1\cdot\boldsymbol{x}} & \\ \qquad + D_2\begin{pmatrix}\sqrt{A_+(p)}\\ -\sqrt{A_-(p)}\end{pmatrix} e^{-i\boldsymbol{p}_2^{\text{refl.}}\cdot\boldsymbol{x}} + D_1\begin{pmatrix}\sqrt{A_-(p)}\\ \sqrt{A_+(p)}\end{pmatrix} e^{-i\boldsymbol{p}_1^{\text{refl.}}\cdot\boldsymbol{x}} & \text{for } d > x > d+l\,, \\ E_2\begin{pmatrix}1\\0\end{pmatrix} e^{i\boldsymbol{p}_2^0\cdot\boldsymbol{x}} + E_1\begin{pmatrix}0\\1\end{pmatrix} e^{i\boldsymbol{p}_1^0\cdot\boldsymbol{x}} + F_2\begin{pmatrix}1\\0\end{pmatrix} e^{-i\boldsymbol{p}_2^{0,\text{refl.}}\cdot\boldsymbol{x}} + F_1\begin{pmatrix}0\\1\end{pmatrix} e^{-i\boldsymbol{p}_1^{0,\text{refl.}}\cdot\boldsymbol{x}} & \text{for } x > d+l\,. \end{cases} \tag{66}$$

In order to determine the transmitted part of the wave function, we have to calculate $\begin{pmatrix}E_2\\E_1\end{pmatrix}$ in terms of $\begin{pmatrix}A_2\\A_1\end{pmatrix}$.

Using again the boundary conditions, we get eight equations which can be used to eliminate the four quantities $C_{1,2}$ and $D_{1,2}$ and to relate $A_{1,2}$ and $B_{1,2}$ to $E_{1,2}$. In addition to Eqn. (42), we get

$$\mathbb{M}_{d'}\begin{pmatrix}\mathcal{C}\\ \mathcal{D}\end{pmatrix} = \mathbb{M}_{d'}^{(0)}\begin{pmatrix}\mathcal{E}\\ \mathcal{F}\end{pmatrix}. \tag{67}$$

This yields

$$\begin{pmatrix}\mathcal{E}\\ \mathcal{F}\end{pmatrix} = (\mathbb{M}_{d'}^{(0)})^{-1}\,\mathbb{M}_{d'}\mathbb{M}_d^{-1}(\mathbb{M}_d^{(0)})\begin{pmatrix}\mathcal{A}\\ \mathcal{B}\end{pmatrix} = \begin{pmatrix}\mathcal{M}_{11} & \mathcal{M}_{12}\\ \mathcal{M}_{21} & \mathcal{M}_{22}\end{pmatrix}\begin{pmatrix}\mathcal{A}\\ \mathcal{B}\end{pmatrix} \tag{68}$$

where each $\mathcal{M}_{ij}$ is a 2×2–matrix. If we apply the additional boundary condition $\mathcal{F} = 0$ (no atoms from the right), we get a relation between $\mathcal{A}$ and $\mathcal{E}$ as well as between $\mathcal{B}$ and $\mathcal{A}$:

$$\mathcal{B} = -\mathcal{M}_{22}^{-1}\mathcal{M}_{21}\mathcal{A} =: \mathcal{R}\mathcal{A}\,, \tag{69}$$

$$\mathcal{E} = (\mathcal{M}_{11} - \mathcal{M}_{12}\mathcal{M}_{22}^{-1}\mathcal{M}_{21})\mathcal{A} =: \mathcal{T}\mathcal{A}\,. \tag{70}$$

This determines the amplitudes of the outgoing and the reflected wave function.

The 2×2–matrices

$$\mathcal{T} = \begin{pmatrix}T_{22} & T_{21}\\ T_{12} & T_{11}\end{pmatrix} \quad \text{and} \quad \mathcal{R} = \begin{pmatrix}R_{22} & R_{21}\\ R_{12} & R_{11}\end{pmatrix} \tag{71}$$

are the *transmission* and the *reflection matrix*, respectively. If the incoming atomic beam consists of atoms in the ground state, then $|T_{11}|^2$ and $|T_{21}|^2$ are the probabilities to find the transmitted atom in the ground state, or in the excited state, respectively. If the incoming atoms are in an excited state, then $|T_{12}|^2$ and $|T_{22}|^2$ are the probabilities to find the transmitted atom in the ground state or on the excited state, respectively. The analogous holds for the reflection matrix $\mathcal{R}$.

Note that these quantities are *not* normalised to one: In the first case of incoming ground state atoms, we have from current conservation

$$(1-|R_{11}|^2)\,p_1^0-|R_{21}|^2\,p_2^0=|T_{11}|^2\,p_1^0+|T_{21}|^2\,p_2^0\,. \tag{72}$$

From this we get

$$1=|T_{11}|^2+|T_{21}|^2\,\frac{p_2^0}{p_1^0}+|R_{11}|^2+|R_{21}|^2\,\frac{p_2^0}{p_1^0} \tag{73}$$

and, especially,

$$|T_{11}|^2+|T_{21}|^2\,\frac{p_{02}}{p_1^0}\le 1,\qquad |R_{11}|^2+|R_{21}|^2\,\frac{p_2^0}{p_1^0}\le 1\,. \tag{74}$$

If the incoming atoms are in the excited state, we get instead

$$1=|T_{12}|^2\,\frac{p_1^0}{p_2^0}+|T_{22}|^2+|R_{12}|^2\,\frac{p_1^0}{p_2^0}+|R_{22}|^2\,. \tag{75}$$

4.2 Beam splitting by transmission

For the components of the matrix $\mathcal{T}$ we get

$$\begin{aligned} T_{11} &= \frac{1}{Z}\,p_1^0[A_-p_2(2p_2^0p_1\cos(lp_1)-i((p_2^0)^2+p_1^2)\sin(lp_1)) \\ &\quad + A_+p_1(2p_2^0p_2\cos(lp_2)-i((p_2^0)^2+p_2^2)\sin(lp_2))]\,, \end{aligned} \tag{76}$$

$$\begin{aligned} T_{12} &= \frac{1}{Z}\,\sqrt{A_-A_+}\,p_2^0\big[p_1p_2(p_2^0+p_1^0)\,(\cos(lp_2)-\cos(lp_1)) \\ &\quad + ip_2(p_1^2+p_1^0p_2^0)\sin(lp_1)-ip_1(p_2^2+p_1^0p_2^0)\sin(lp_2)]\,, \end{aligned} \tag{77}$$

$$\begin{aligned} T_{21} &= \frac{1}{Z}\,\sqrt{A_-A_+}\,p_1^0\big[p_1p_2(p_1^0+p_2^0)\,(\cos(lp_2)-\cos(lp_1)) \\ &\quad + ip_2(p_1^0p_2^0+p_1^2)\sin(lp_1)-ip_1(p_1^0p_2^0+p_2^2)\sin(lp_2)]\,, \end{aligned} \tag{78}$$

$$\begin{aligned} T_{22} &= \frac{1}{Z}\,p_2^0[A_+p_2(2p_1^0p_1\cos(lp_1)-i((p_1^0)^2+p_1^2)\sin(p_1l)). \\ &\quad + A_-p_1(2p_1^0p_2\cos(lp_2)-i((p_1^0)^2+p_2^2)\sin(lp_2))]\,, \end{aligned} \tag{79}$$

with

$$\begin{aligned} Z &= -A_-A_+(p_1^0-p_2^0)^2\,p_1p_2 \\ &\quad + p_1\cos(lp_1)[(2(A_-^2+A_+^2)\,p_1^0p_2^0+A_-A_+(p_1^0+p_2^0)^2)\,p_2\cos(lp_2) \\ &\quad - i(A_-p_2^0((p_1^0)^2+p_2^2)+A_+p_1^0((p_2^0)^2+p_2^2))\sin(lp_2)] \\ &\quad - \sin(lp_1)\,[i(A_+p_2^0((p_1^0)^2+p_1^2)+A_-p_1^0((p_2^0)^2+p_1^2))\,p_2\cos(lp_2). \\ &\quad + \tfrac{1}{2}(A_-^2((p_2^0)^2+p_1^2)\,((p_1^0)^2+p_2^2)+2A_-A_+(p_1^0p_2^0+p_1^2)\,(p_1^0p_2^0+p_2^2). \\ &\quad + A_+^2((p_1^0)^2+p_1^2)\,((p_2^0)^2+p_2^2))\sin(lp_2)]\,. \end{aligned} \tag{80}$$

For vanishing laser beam, that is, for $\Omega_{ba} = 0$ (which gives $A_+ = 1$, $A_- = 0$, $p_{1,2} = p^0_{1,2}$), the off-diagonal terms vanish, and we have $T_{11} = e^{ip^0_1 l}$ and $T_{22} = e^{ip^0_2 l}$. The above matrix elements possess a structure similar to the corresponding text book results of the plane wave scattering by a rectangular potential barrier.

We plot the probabilities $|T_{11}|^2$ and $|T_{21}|^2$ and their weighted sum $|T_{11}|^2 + \frac{p^0_2}{p^0_1} |T_{21}|^2$ for various cases in order to demonstrate the main features of the transmission. The actual values for $|T_{11}|^2$ and $|T_{21}|^2$ depend on the momentum of the excited incoming atom p^0_1, on the strength of the laser beam characterized by Ω_{ba}, on the width of the laser region l, and on the quantity y which can be manipulated by the detuning. Owing to this set of quantities which influence the measured probabilities we discuss several cases:

1. In this first case we vary the momentum, or the energy, of the incoming ground state atom, see Fig. 9. We plot the probabilities $|T_{11}|^2$ (dotted curve) and $|T_{21}|^2$ (dashed curve) and their weighted sum (solid curve). Similar to the case of the scattering of a one-level plane wave at a constant potential barrier, the total outgoing intensity for low energies is very small. If the energy of the incoming atom is comparable to the potential barrier, then the intensity grows and displays some oscillations. For large energies it approaches unity. However, in our case the transmission shows more structure: while the weighted sum $|T_{11}|^2 + \frac{p^0_2}{p^0_1}|T_{21}|^2$ asymptotically tends to unity, the probabilities $|T_{11}|^2$ and $|T_{21}|^2$ oscillate with an increasing period and the strength and the period of these oscillations depend on the parameter y.
2. In the next case we fix the momentum p^0_1 of the incoming atom, the strength of the barrier Ω_{ba} and the parameter y connected with the detuning. The variable

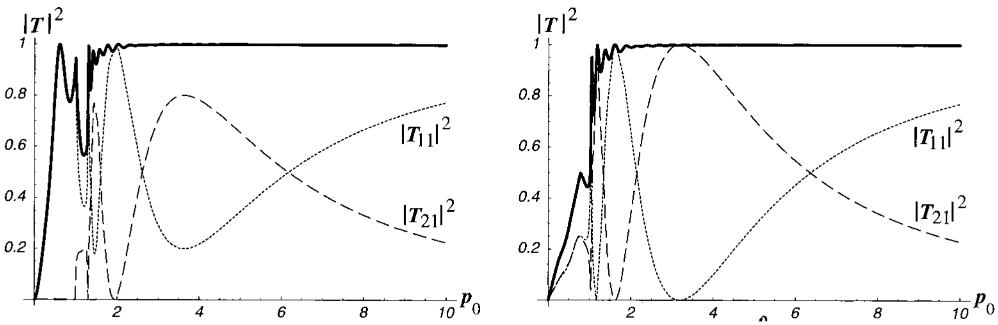

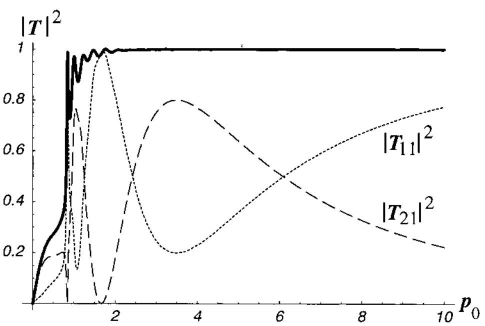

Fig. 9 Display of the probabilities $|T_{11}|^2$ (dotted curve) and $|T_{21}|^2$ (dashed curve) and the sum $|T_{11}|^2 + \frac{p^0_2}{p^0_1}|T_{21}|^2$ (solid curve) as function of the momentum of the incoming atom in the ground state in the case of resonance $y = 0$ (upper right diagram), for $y = 0.5$ (upper left diagram), and $y = -0.5$ (lower diagram). The fixed parameters are $m\hbar\Omega_{ba} = 0.4$, $l/\hbar = 15$ in arbitrary units.

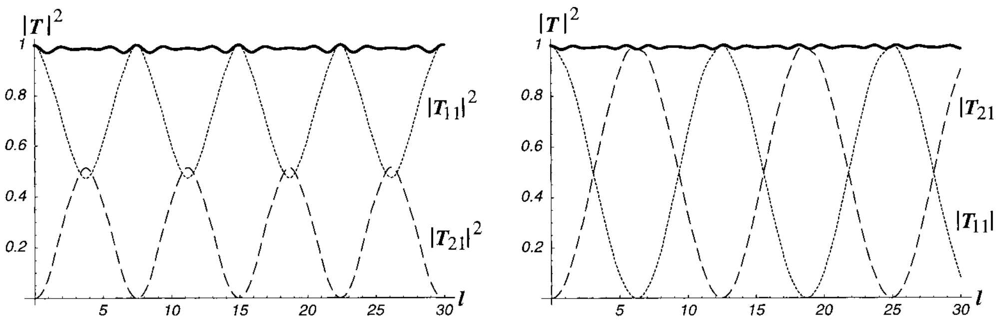

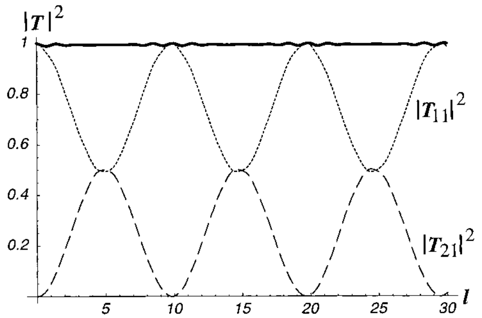

Fig. 10 The functions $|T_{11}|^2$, $|T_{21}|^2$, and $|T_{11}|^2 + \frac{p_2^0}{p_1^0}|T_{21}|^2$ as function of the width $l/\hbar$ of the laser beam in the case of resonance $y = 0$ (upper right), and for $y = 1$ (upper left), and $y = -1$ (lower). The parameters are $p_1^0 = 1.5$, $y = 0$, and $m\hbar\Omega_{ba} = 0.4$ in arbitrary units.

parameter is the width l of the laser barrier. The corresponding diagrams in Fig. 10 show the spatial version of the Rabi oscillations. Similar to the usual Rabi oscillations in time, the wavelength of the spatial Rabi oscillations as well as the population transfer decrease for increasing $|y|$. Wavelength and population transfer are maximal for resonance $y = 0$ and decrease for increasing $|y|$.

3. Now we fix the energy p_1^0, the length l, and the parameter y and vary the strength of the barrier Ω_{ba} connected with the power of the laser beam, see Fig. 11. This type of experiment has been carried out by Bordé *et al.* [16] and Ekstrom *et al.* [17] for large kinetic energy of the atoms compared with the Rabi energy $\hbar\Omega_{ba}$. The corresponding diagrams show first an oscillatory behavior for the excited and ground states leaving the laser region while the total

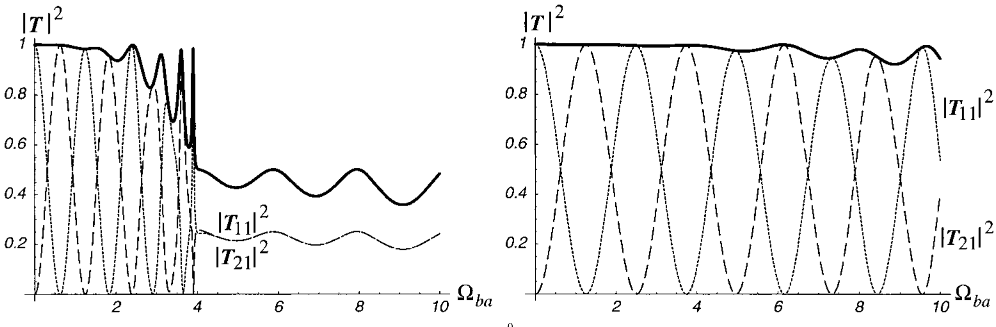

Fig. 11 The functions $|T_{11}|^2$, $|T_{21}|^2$, and $|T_{11}|^2 + \frac{p_2^0}{p_1^0}|T_{21}|^2$ as function of the Rabi frequency $m\hbar\Omega_{ba}$ of the laser beam in the case of resonance $y = 0$. The parameters are $p_1^0 = 2$, $y = 0$, and $l/\hbar = 15$. Right: Same as left but with $p_1^0 = 4$.

intensity is almost unity. This corresponds to the probability $|T_{21}|^2 = \sin(k_R l) = \sin(m\Omega_{ba} l/p_0)$ connected with the case of a small barrier or high kinetic energies (compare the approximation (98)). This behavior changes drastically if the potential barrier given by Ω_{ba} is comparable to the kinetic energy of the incoming atom: the oscillations die out and most of the atoms are reflected. In addition, a non-zero y damps the population transfer.

After leaving the laser zone, the atomic waves again have momenta $\boldsymbol{p}_1^0$ and $\boldsymbol{p}_2^0 + \hbar\boldsymbol{k}$. The two momenta $\boldsymbol{p}_1^0$ and $\boldsymbol{p}_2^0$ are different which leads to an extra momentum of the second beam in normal direction, so that in general the atomic waves are scattered inelastically. This extra momentum is supplied by the detuning of the laser beam and gives rise to the Rabi oscillations.

4.3 The reflection

The components of the reflection matrix are given by

$$\begin{aligned} R_{11} = \frac{1}{Z}\{ & 2A_-A_+(p_1^0 - p_2^0)(p_1^0 + p_2^0)p_1p_2 \\ & + 2A_-p_1\cos(lp_1)[A_+(p_2^0 - p_1^0)(p_1^0 + p_2^0)p_2\cos(lp_2) \\ & + ip_2^0(p_1^0 - p_2)(p_1^0 + p_2)\sin(lp_2)] \\ & + \sin(lp_1)[2iA_+p_2^0(p_1^0 - p_1)(p_1^0 + p_1)p_2\cos(lp_2) \\ & + (A_-^2((p_2^0)^2 + p_1^2)(p_1^0 - p_2)(p_1^0 + p_2) + 2A_-A_+(p_1^0p_2^0 - p_1p_2)(p_1^0p_2^0 + p_1p_2) \\ & + A_+^2(p_1^0 - p_1)(p_1^0 + p_1)((p_2^0)^2 + p_2^2))\sin(lp_2)\}, \end{aligned} \tag{81}$$

$$\begin{aligned} R_{12} = -\frac{2}{Z}\sqrt{A_-A_+}\,p_1^0\{ & (A_+ - A_-)(p_1^0 - p_2^0)p_1p_2 \\ & + p_1\cos(lp_1)[(A_- - A_+)(p_1^0 - p_2^0)p_2\cos(lp_2) + i(p_1^0p_2^0 - p_2^2)\sin(lp_2)] \\ & + \sin(lp_1)[i(p_1^2 - p_1^0p_2^0)p_2\cos(lp_2) \\ & + ((A_-p_1^0 + A_+p_2^0)p_1^2 - (A_+p_1^0 + A_-p_2^0)p_2^2)\sin(lp_2)]\}, \end{aligned} \tag{82}$$

$$\begin{aligned} R_{21} = -\frac{2}{Z}\sqrt{A_-A_+}\,p_1^0\{ & (A_+ - A_-)(p_1^0 - p_2^0)p_1p_2 \\ & + p_1\cos(lp_1)[(A_- - A_+)(p_1^0 - p_2^0)p_2\cos(lp_2) + i(p_1^0p_2^0 - p_2^2)\sin(lp_2)] \\ & + \sin(lp_1)[i(p_1^2 - p_1^0p_2^0)p_2\cos(lp_2) \\ & + ((A_-p_1^0 + A_+p_2^0)p_1^2 - (A_+p_1^0 + A_-p_2^0)p_2^2)\sin(lp_2)]\}, \end{aligned} \tag{83}$$

$$\begin{aligned} R_{22} = -\frac{1}{Z}\{ & 2A_-A_+(p_1^0 - p_2^0)(p_1^0 + p_2^0)p_1p_2 \\ & + 2A_+p_1\cos(lp_1)[A_-(p_2^0 - p_1^0)(p_1^0 + p_2^0)p_2\cos(lp_2) \\ & - ip_1^0(p_2^0 - p_2)(p_2^0 + p_2)\sin(lp_2)] \\ & + \sin(lp_1)[-2iA_-p_1^0(p_2^0 - p_1)(p_2^0 + p_1)p_2\cos(lp_2) \\ & - (A_+^2((p_1^0)^2 + p_1^2)(p_2^0 - p_2)(p_2^0 + p_2) + 2A_-A_+(p_1^0p_2^0 - p_1p_2)(p_1^0p_2^0 + p_1p_2) \\ & + A_-^2(p_2^0 - p_1)(p_2^0 + p_1)((p_1^0)^2 + p_2^2))\sin(lp_2)]\}, \end{aligned} \tag{84}$$

with

$$
\begin{aligned}
Z = {} & 2A_-A_+(p_1^0 - p_2^0)^2 p_1 p_2 + 2p_1 \cos(lp_1)\,[-(2A_-^2 p_1^0 p_2^0 + 2A_+^2 p_1^0 p_2^0 \\
& + A_-A_+(p_1^0 + p_2^0)^2)\, p_2 \cos(lp_2) \\
& + i(A_- p_2^0((p_1^0)^2 + p_2^2) + A_+ p_1^0((p_2^0)^2 + p_2^2)) \sin(lp_2)] \\
& + \sin(lp_1)\ [2i(A_+ p_2^0((p_1^0)^2 + p_1^2) + A_- p_1^0((p_2^0)^2 + p_1^2))\, p_2 \cos(lp_2) \\
& + (A_-^2((p_2^0)^2 + p_1^2)((p_1^0)^2 + p_2^2) + 2A_-A_+(p_1^0 p_2^0 + p_1^2)(p_1^0 p_2^0 + p_2^2) \\
& + A_+^2((p_1^0)^2 + p_1^2)((p_2^0)^2 + p_2^2)) \sin(lp_2)]\,. \qquad (85)
\end{aligned}
$$

For atomic *mirrors* one would like to have an almost perfect reflection, that is, $\mathcal{R} \approx 1$. Since the reflected wave also always consists in both kinds of atoms, this device may also be used for the beam splitting. The reflected wave is non–negligible only for small momenta p_x. Therefore, provided one prepares atoms with momenta which have a very small angle with the surface of the laser beam, or one uses very strong laser fields, then the reflection can be used as beam splitter or as a mirror for very cold atoms. Inspection of the above result shows immediatley that the reflection matrix vanishes for vanishing laser power (see also the approximation in Sec. 5.4). Usually the reflected waves can be neglected.

The graphs describing the reflected waves are complementary to that for the transmitted wave. We show, for convenience, diagrams where the reflection coefficients are displayed as functions of p_1^0, l, and Ω_{ba}, respectively, see Fig. 12. Most atoms are reflected in the case where the kinetic energy is smaller than the interaction energy, as can be seen from the upper and lower diagrams in Fig. 12. From the middle diagram we discover that the reflection has only a periodic dependence on the width of the laser region.

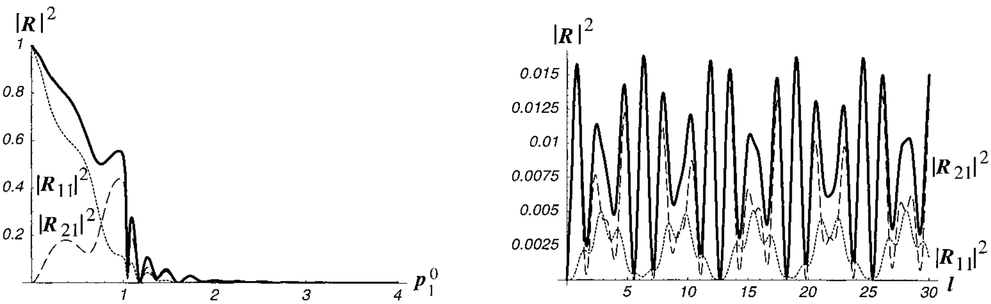

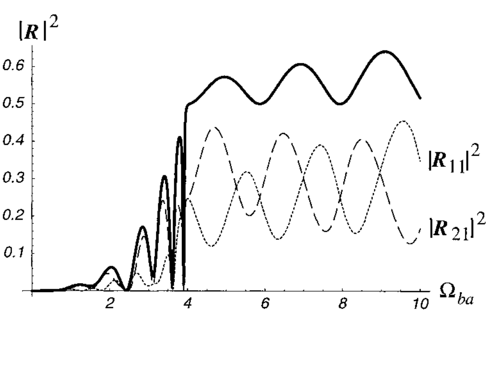

Fig. 12 The reflection coefficients $|R_{11}|^2$, $|R_{21}|^2$, and the weighted sum $|R_{11}|^2 + \frac{p_2^0}{p_1^0}|R_{21}|^2$ as functions of p_1^0 (upper left diagram), of l (upper right diagram), and of Ω_{ba} (lower diagram). Note the different scales as compared to the diagrams of the transmission coefficients.

Of course, the weighted sums of transmission coefficients as well as of the reflection coefficients add up to unity, in accordance to relation (73).

4.4 The Borrmann effect with reflected wave

The exit boundary of the laser region influences the wave function inside the laser region and thus the condition for the Borrmann effect. If we take these waves into account, then we have to calculate the current inside the laser region from (66). We get, instead of (44),

$$\begin{aligned} j_z &= -\frac{i\hbar}{2m}\left(\psi_b^*\,\partial_z\psi_b - \partial_z\psi_b^*\,\psi_b + \psi_a^*\,\partial_z\psi_a - \partial_z\psi_a^*\,\psi_a\right) \\ &= \frac{\hbar}{m}\left(\left(A_-\,|C_1|^2 + A_+\,|C_2|^2 + A_-\,|D_1|^2 + A_+\,|D_2|^2\right)(p_z + \hbar k)\right. \\ &\quad \left. + \left(A_+\,|C_1|^2 + A_-\,|C_2|^2 + A_+\,|D_1|^2 + A_-\,|D_2|^2\right)p_z + \text{oscillatory terms}\right). \end{aligned} \tag{86}$$

The condition for the Borrmann effect is again $\langle j_z \rangle = 0$ which yields

$$p_z = -\frac{A_-(|C_1|^2 + |D_1|^2) + A_+(|C_2|^2 + |D_2|^2)}{|C_2|^2 + |D_2|^2 + |C_1|^2 + |D_1|^2}\,\hbar k \tag{87}$$

indicating the additional influence of the beam which is reflected at the exit surface. If we neglect the wave which is reflected at the exit boundary, then we recover the results of Sec. 3.3. Since the exact evaluation of the above expression is not very illuminating, we refer to the approximation in Sec. 5.1.

In the same way one can easily calculate the currents $\boldsymbol{j}_1$, $\boldsymbol{j}_2$, $\boldsymbol{j}_b$, and $\boldsymbol{j}_a$ and the conditions for the other two versions of a Borrmann effect.

5 An approximation for fast atoms

If the atoms possess a large kinetic energy as compared to the potential energy provided by the interaction of the two-level atom with the laser beam, we can perform a useful approximation. The validity of this approximation is characterised by the ratio

$$\kappa = \frac{E_{\text{Rabi}}}{E_{\text{kin}}} = \frac{\hbar\Omega_{ba}}{p^2/(2m)}\,. \tag{88}$$

In this case we can expand the square roots in (37) and (38) and find

$$p_{n1,2} \approx p^0_{n,1} - \frac{m\hbar\Omega_{ba}}{p^0_{n,1}}\left(y(\boldsymbol{p}) \mp \sqrt{1 + y^2(\boldsymbol{p})}\right), \tag{89}$$

or

$$p_{n1,2} \approx p^0_{n,2} + \frac{m\hbar\Omega_{21}}{p^0_{n,2}}\left(y(\boldsymbol{p}) \pm \sqrt{1 + y^2(\boldsymbol{p})}\right). \tag{90}$$

With the same approximations we also find

$$\delta p(\boldsymbol{p}) := p_{n1}^0 - p_{n2}^0 \approx \frac{m\hbar\Omega_{21} y(\boldsymbol{p})}{p_{n2}^0} \approx \frac{m\hbar\Omega_{21} y(\boldsymbol{p})}{p_{n1}^0} \,. \tag{91}$$

5.1 The Borrmann effect

If we use this approximation for the results (56, 57) of the first case (the other two cases gave exact results), then we find the following:

1. For incoming atoms in the ground state we use (56) and get to first order

   $$p_z = -\frac{1}{2}\,\frac{1}{1+y^2}\left(1+\frac{\kappa}{2}\right)\hbar k \,. \tag{92}$$

   The zeroth order result $p_z = -\frac{1}{2}\frac{1}{1+y^2}\,\hbar k$ coincides with that in neutron optics [10]. If the tangential part of the incoming beam is in $\boldsymbol{k}$-direction, $\boldsymbol{p}_t^0 \sim \boldsymbol{k}$, then the incident angle is

   $$\tan\theta = \frac{p_z}{p_1^0} = -\frac{1}{2}\,\frac{1}{1+y^2}\left(1+\frac{\kappa}{2}\right)\frac{\hbar k}{p_1^0} \,. \tag{93}$$

   This angle depends on the wave vector k of the laser bam, via y on the detuning Δ, and the kinetic energy of the incoming atom. The incident angle is maximal in the case of resonance.
2. For an incoming atomic beam in the excited state we use (57) and get to first order

   $$p_z + \hbar k = \frac{1}{2}\,\frac{1}{1+y^2}\left(1-\frac{\kappa}{2}\right)\hbar k \tag{94}$$

   and a corresponding incidence angle

   $$\tan\theta = \frac{p_z+\hbar k}{p_2^0} = \frac{1}{2}\,\frac{1}{1+y^2}\left(1-\frac{\kappa}{2}\right)\frac{\hbar k}{p_2^0} \,. \tag{95}$$

We find the same result for the Borrmann effects which take into account the reflected waves, see Section 4.4. Therefore the reflected waves contribute to the corresponding incidence angle at most to second order of κ.

The incidence angle is different for excited and ground state atoms. To zeroth order, the angle for the incoming excited atoms is just opposite to that for the ground state atoms. To first order, an asymmetry comes in, both beams have additional parts in the same direction.

5.2 The pendellösung

In the present approximation, the wavelength of the *pendellösung* effect is

$$\lambda_{\text{Pendel}} = 2\pi\,\frac{p_1^0}{m\Omega_{ba}}\,\frac{1}{\sqrt{1+y^2}} \,. \tag{125}$$

This wavelength increases with the kinetic energy of the atoms and for smaller laser power. It can also be varied with the detuning; it is maximal for resonance.

5.3 *Beam splitting by transmission*

If we expand to first order in $\hbar\Omega_{ba}m/(p_1^0)^2$ the phase as well as the amplitude, we get from (76–79) the transmission matrix

$$T_{11} = e^{i(p_1^0-\delta p)\,l}\left(\cos(k_R l) + \frac{iy}{\sqrt{1+y^2}}\,\sin(k_R l)\right), \tag{97}$$

$$T_{12} = e^{i(p_1^0-\delta p)\,l}\,\frac{i}{\sqrt{1+y^2}}\left(1 - \frac{m\hbar\Omega}{(p_1^0)^2}\,y\right)\sin(k_R l), \tag{98}$$

$$T_{21} = e^{i(p_1^0-\delta pa)\,l}\,\frac{i}{\sqrt{1+y^2}}\left(1 + \frac{m\hbar\Omega}{(p_1^0)^2}\,y\right)\sin(k_R l), \tag{99}$$

$$T_{22} = e^{i(p_1^0-\delta p)\,l}\left(\cos(k_R l) - \frac{iy}{\sqrt{1+y^2}}\,\sin(k_R l)\right), \tag{100}$$

where we defined the *Rabi wavelength*

$$k_R = \frac{m\Omega_{ba}}{p_1^0}\,\sqrt{1+y^2} \tag{101}$$

and used δp from (91). In this approximation, the population transfer between atoms in the excited and the ground state is exactly sinusoidal. For example, $|T_{11}|^2 = 1 - \frac{1}{1+y^2}\sin^2(k_R l)$ which, in the case of $y = 0$, reduces to $|T_{11}|^2 = \cos^2(m\Omega_{ba}l/p_1^0)$.

The Ω_{ba}-dependent amplitudes in the off-diagonal terms indicate that, even in this approximation, a reflection appears. However, amplitude effects are much smaller than oscillatory effects. Thus, for most purposes one can neglect these Ω_{ba}-terms in the amplitudes. In this case, the structure of the above result is analogous to the result of the beam splitting process with laser pulses in the time domain. One gets the latter result by replacing $k_R l$ by $\Omega_R t$ where t is the duration of the laser pulse and Ω_R the corresponding Rabi frequency. Since the latter is given by $\Omega_R = \Omega_{ba}\sqrt{1+y^2}$, we have, by comparison, $\Omega_R = v_1^0 k_R$, with $v_1^0 = p_1^0/m$.

5.4 *Reflection*

Using the same approximation, we get for the reflection matrix

$$R_{11} = \frac{\hbar_m\Omega_{ba}}{2(p_1^0)^2}\,e^{2i(p_1^0-\delta p)\,l}\,e^{ik_R l}\,\frac{i\sin(k_R l)}{\sqrt{1+y^2}}, \tag{102}$$

$$R_{12} = \frac{\hbar_m\Omega_{ba}}{4(p_1^0)^2}\left(-1 + e^{2i(p_1^0-\delta p)\,l}\,\frac{y^2+\cos(2k_R l)}{1+y^2}\right), \tag{103}$$

$$R_{21} = \frac{\hbar_m\Omega_{ba}}{4(p_1^0)^2}\left(-1 + e^{2i(p_1^0-\delta p)\,l}\,\frac{y^2+\cos(2k_R l)}{1+y^2}\right), \tag{104}$$

$$R_{22} = \frac{\hbar_m\Omega_{ba}}{2(p_1^0)^2}\,e^{2i(p_1^0-\delta p)\,l}\,e^{-ik_R l}\,\frac{i\sin(k_R l)}{\sqrt{1+y^2}}. \tag{105}$$

Of course, this matrix vanishes for vanishing laser power or for large kinetic energy of the incoming atoms ($\kappa \to 0$).

6 Discussion

We have calculated the exact results for the scattering of a two-level system at a periodic potential. Since this is a stationary problem, the structure of the result is in general different from the interaction of a two-level system with a laser pulse which is a time-dependent interaction. We presented the transition matrix which describes the probability to find the atom behind the laser beam in an upper or lower state for an incoming atom which is either in the lower or upper state, too. Also the reflection matrix has been given. The total intensity shows a similar behaviour to that of the intensity obtained from the scattering of a one-level system scattered at a usual potential barrier. However, this total intensity is the sum of intensities belonging to the upper and lower state which oscillate.

For atom interferometers one uses π- and $\pi/2$-beams, see Fig. 13, e.g., for a simple realisation. These beams are defined by their action on the population of the incoming atom beam: The π-beam reverses the population while a $\pi/2$-beam splits the population with a 50:50 probability. As one can easily see from the probabilities plotted, this is only possible for $y = 0$. A π-beam is a configuration where the function $|T_{11}|^2$ (the dotted curve in Figs. 9, 10, and 11) has the value 0 (in this case the $|T_{21}|^2$ – the dashed curve – has a value smaller than 1 because one has to take the reflected part into consideration). A $\pi/2$-pulse represents a configuration where the functions $|T_{11}|^2$ and $|T_{21}|^2$ are equal. In this case the dotted and the dashed curves in Figs. 9, 10, and 11 cross each

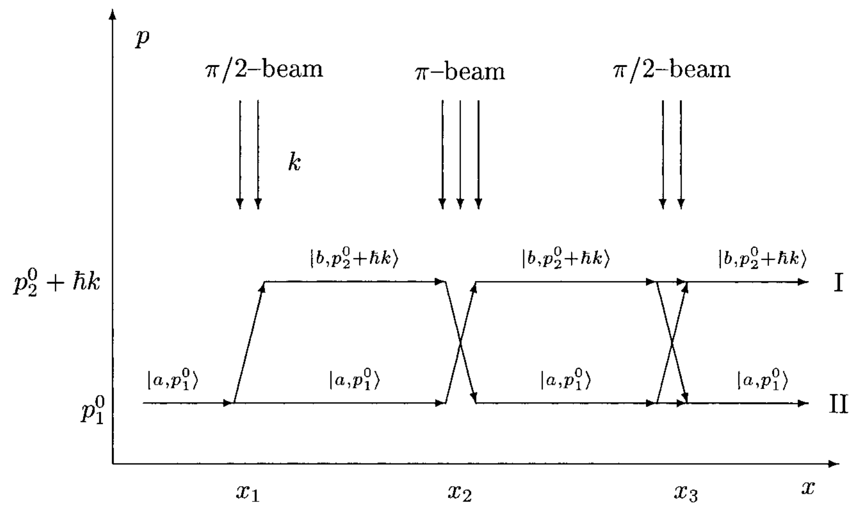

Fig. 13 A Ramsey-Bordé-interferometer in the position-momentum representation. The incoming atoms $|a, p_1^0\rangle$ are in the ground state and have a momentum p_1^0. The $\pi/2$-beam acts as state splitter leading to a superposition of the incoming state and excited states $|b, p_2^0 + \hbar k\rangle$ with momentum $p_2^0 + \hbar k$, and the π-beam reverses the states. The atomic interference pattern can be read off from port I or port II. Note that except for $y = 0$ the two momenta p_1^0 and p_2^0 are different.

other. In the case of large kinetic energy compared to the potential energy of the laser beam, a π-beam is given by $|T_{11}|^2 = 0$, $|T_{21}|^2 = 1$, and a $\pi/2$-beam by $|T_{11}|^2 = |T_{21}|^2 = 1/2$. Thus, we have for a π-beam $k_R l = \pi/2$ and for a $\pi/2$-beam $k_R l = \pi/4$. In the case of an incoming atomic beam with fixed kinetic energy, these conditions can be obtained by either varying the width or the power of the laser beam.

It has to be mentioned that the two momenta p_1^0 and p_2^0 are different for $y \neq 0$. (An analogue effect takes place in the time domain when operating with laser pulses. In this case one has a constant and fixed momentum but two different energies.) These two momenta do not influence the interference pattern for a symmetrical interferometer geometry. However, in a trapezian geometry, for example, they contribute to the interference pattern [18, 7].

The calculations of above can be applied to the beam splitting process in a gravitational field. In this case the additional gravitational acceleration modifies the condition $y = 0$ so that the resonance condition is no longer fulfilled. Consequently, first a π- or $\pi/2$-beam as defined in in the case of free gravity loses this property, and secondy there may be more contributions to the reflected beam. This will be treated in a forthcoming paper [15].

C.L. would like to thank Ch. J. Bordé and Ch. Chardonnet for their hospitality at the Laboratoire de Physique des Lasers at the Université Paris 13 and the CNRS (France) for the financial support.

Appendix: Group velocity and current

Theorem: The currents $\boldsymbol{j}_{1,2} = -\frac{i\hbar}{2m}\,(\psi_{1,2}^+ \nabla \psi_{1,2} - \nabla \psi_{1,2}^+ \psi_{1,2}$ are proportional to the group velocities $\boldsymbol{v}_{1,2}$:

Proof: The matrix equation (14) has the general form $\mathcal{A}(p)\, a = 0$ and leads to the solvability condition $\det \mathcal{A}(\boldsymbol{x}, \boldsymbol{p}) = 0$. In our case this condition is $(E - f_1(\boldsymbol{x}, \boldsymbol{p}))\,(E - f_2(\boldsymbol{x}, \boldsymbol{p})) = 0$ so that either $E - f_1(\boldsymbol{x}, \boldsymbol{p}) = 0$ or $E - f_2(\boldsymbol{x}, \boldsymbol{p}) = 0$ with the corresponding solutions $\boldsymbol{p}_1$ and $\boldsymbol{p}_2$. If one of these conditions, say the first one, is fulfilled, then there exists an eigenvector a_1 so that $\mathcal{A}(\boldsymbol{x}, \boldsymbol{p}_1)\, a_1(\boldsymbol{p}_1) = 0$. In other words: $E - f_1(\boldsymbol{x}, \boldsymbol{p}_1) = 0 \Leftrightarrow \mathcal{A}(\boldsymbol{x}, \boldsymbol{p}_1)\, a_1(\boldsymbol{p}_1) = 0$. This implies that on the mass shell

$$\frac{\partial f_1(\boldsymbol{x}, \boldsymbol{p}_1)}{\partial p_1}\, d\boldsymbol{p}_1 = 0 \Leftrightarrow \frac{\partial \mathcal{A}(\boldsymbol{x}, \boldsymbol{p}_1)}{\partial p_1}\, d\boldsymbol{p}_1\, a_1(\boldsymbol{p}_1) + \mathcal{A}(\boldsymbol{x}, \boldsymbol{p}_1)\, \frac{\partial a_1(p_1)}{\partial p_1}\, d\boldsymbol{p}_1 = 0\,. \tag{106}$$

Since $\mathcal{A}(\boldsymbol{x}, \boldsymbol{p})$ is a symmetric matrix we have also $(a_1(\boldsymbol{p}_1))^+ \mathcal{A}(\boldsymbol{x}, \boldsymbol{p}_1) = 0$. Therefore the right-hand-condition gives $(a_1(\boldsymbol{p}_1))^+ \frac{\partial \mathcal{A}(\boldsymbol{x}, \boldsymbol{p}_1)}{\partial p_1}\, a^+(\boldsymbol{p}_1)\, d\boldsymbol{p}_1 = 0$. Because $\boldsymbol{p}_1$ is the only independent variable and $\frac{\partial f_1(\boldsymbol{x}, \boldsymbol{p}_1)}{\partial p_1}\, d\boldsymbol{p}_1 = 0$ as well as $(a_1(p_1))^+ \frac{\partial \mathcal{A}(p_1)}{\partial p_1}\, a_1(\boldsymbol{p}^+)\, d\boldsymbol{p}_1 = 0$ are scalar conditions which hold on the mass shell $E - f_1(\boldsymbol{p}_1, \boldsymbol{x}) = 0$, it follows that

$$\nabla_p f_1(\boldsymbol{x}, \boldsymbol{p}_1) \sim (a_1(\boldsymbol{p}_1))^+ \nabla_p \mathcal{A}(\boldsymbol{x}, \boldsymbol{p}_1)\, a_1(\boldsymbol{p}_1)\,. \tag{107}$$

The same is true for the second mass shell $E - f_2(\boldsymbol{x}, \boldsymbol{p}_2) = 0$.[1]

References

[1] M. Kasevich and S. Chu, Atomic interferometry using stimulated Raman transitions. Phys. Rev. Lett. **67** (1991) 181
[2] F. Riehle, Th. Kisters, A. Witte, J. Helmcke, and Ch. J. Bordé, Optical Ramsey spectroscopy in a rotating frame: Sagnac effect in a matter wave interferometer. Phys. Rev. Lett. **67** (1991) 177
[3] U. Sterr, K. Sengstock, J. H. Müller, D. Bettermann, and W. Ertmer, The magnesium Ramsey interferometer: Applications and prospects. Appl. Phys. B **54** (1992) 341
[4] Ch. J. Bordé, N. Courtier, F. D. Burck, A. N. Goncharov, and M. Gorlicki, Molecular interferometry experiments. Phys. Lett. A **188** (1994) 187
[5] U. Sterr, K. Sengstock, W. Ertmer, F. Riehle, and J. Helmcke. Atom interferometry based on separated light fields. In P. R. Berman, editor, *Atom Interferometry*, page 293 Academic Press, Boston, 1996
[6] Ch. J. Bordé, Atomic interferometry with internal state labeling. Phys. Lett. A **140** (1989) 10
[7] Ch. J. Bordé, Matter wave interferometers: A synthetic approach. In P. R. Berman, editor, *Atom Interferometry*, page 257. Academic Press, Boston, 1996
[8] C. Lämmerzahl and Ch. Bordé, Rabi oscillations in gravitational fields: Exact solution. Phys. Lett. A **203** (1995) 59
[9] P. Marzlin and J. Audretsch, "Freely" falling two-level atom in a running laser wave. Phys. Rev. A **53** (1996) 1004
[10] H. Rauch and D. Petraschek, Dynamical neutron diffraction and its application. In H. Dachs, editor, *Topics in Current Physics*, volume 6, page 303. Springer-Verlag, Berlin, 1978
[11] S. A. Werner, Gravitational and magnetic field effects on the dynamical diffraction of neutrons. Phys. Rev. B **21** (1980) 1774
[12] M. Horne, Neutron interferometry in a gravity field. Physica B **137** (1986) 260
[13] S. A. Werner, H. Kaiser, M. Arif, and R. Clothier, Neutron interference induced by gravity: new results and interpretations. Physica B **151** (1988) 22
[14] U. Bonse and T. Wroblewski, Dynamical diffraction effects in noninertial neutron interferometry. Phys. Rev. D **30** (1984) 1214
[15] C. Lämmerzahl and Ch. J. Bordé, Atomic interferometry in gravitational fields: Influence of gravity on the beam splitter. Gen. Rel. Grav., submitted, 1998
[16] Ch. J. Bordé, S. Avrillier, A. van Lerberghe, C. Salomon, C. Bréant, D. Bassi, and G. Scoles, Observation of optical Ramsey fringes in the 10 μm spectral range using a supersonic beam of SF_6G. Appl. Phys. B **28** (1982) 82
[17] C. R. Ekstrom, C. Kurtsiefer, D. Voigt, O. Dross, T. Pfau, and J. Mlynek, Coherent excitation of a He^* beam observed in atomic momentum distributions. Opt. Comm. **123** (1996) 505
[18] Ch. J. Bordé, Ch. Salomon, S. Avrillier, A. van Lerberghe, Ch. Bréant, D. Bassi, and G. Scoles, Optical Ramsey fringes with travelling waves. Phys. Rev. A **30** (1984) 1836

[1] We can verify this explicitly in our case. We choose $E = f_1(\boldsymbol{x}, \boldsymbol{p})$ and get with

$$\mathcal{A}(\boldsymbol{x}, \boldsymbol{p}) \sim \begin{pmatrix} y(\boldsymbol{x}, \boldsymbol{p}) - \sqrt{1 + y^2(\boldsymbol{x}, \boldsymbol{p})} & -1 \\ -1 & -y(\boldsymbol{x}, \boldsymbol{p}) - \sqrt{1 + y^2(\boldsymbol{x}, \boldsymbol{p})} \end{pmatrix} \tag{108}$$

$$\frac{\partial \mathcal{A}(\boldsymbol{x}, \boldsymbol{p})}{\partial p} = \begin{pmatrix} \dfrac{\partial H(\boldsymbol{x}, \boldsymbol{p} + \hbar \boldsymbol{k})}{\partial p} & 0 \\ 0 & \dfrac{\partial H(\boldsymbol{x}, \boldsymbol{p})}{\partial p} \end{pmatrix} \tag{109}$$

and the solution a from (15) that indeed $a_1^+(\boldsymbol{p})\, \frac{\partial \mathcal{A}(\boldsymbol{x}, \boldsymbol{p})}{\partial p}\, a_1(\boldsymbol{p})$ is proportional to (27).